Chaos

Partial differential equation modeling of rumor propagation in complex networks with higher order of organization

Cite as: Chaos **29**, 053106 (2019); https://doi.org/10.1063/1.5090268
Submitted: 25 January 2019 . Accepted: 15 April 2019 . Published Online: 07 May 2019

Linhe Zhu, Hongyong Zhao, and Haiyan Wang

Chaos ARTICLE scitation.org/journal/cha

Partial differential equation modeling of rumor propagation in complex networks with higher order of organization

Cite as: Chaos **29**, 053106 (2019); doi: 10.1063/1.5090268
Submitted: 25 January 2019 · Accepted: 15 April 2019 ·
Published Online: 7 May 2019

View Online Export Citation CrossMark

Linhe Zhu,[1,2,a)] Hongyong Zhao,[1] and Haiyan Wang[3]

AFFILIATIONS

[1] Department of Mathematics, Nanjing University of Aeronautics and Astronautics, Nanjing 210016, China
[2] Faculty of Science, Jiangsu University, Zhenjiang 212013, China
[3] School of Mathematical and Natural Sciences, Arizona State University, Phoenix, Arizona 85069-7100, USA

[a)] **Electronic mail:** zlhnuaa@126.com

ABSTRACT

Mathematical modeling is an important approach to research rumor propagation in online social networks. Most of prior work about rumor propagation either carried out empirical studies or focus on ordinary differential equation models with only consideration of temporal dimension; little attempt has been given on understanding rumor propagation over both temporal and spatial dimensions. This paper primarily addresses an issue related to how to define a spatial distance in online social networks by clustering and then proposes a partial differential equation model with a time delay to describing rumor propagation over both temporal and spatial dimensions. Theoretical analysis reveals the existence of equilibrium points, *a priori* bound of the solution, the local stability and the global stability of equilibrium points of our rumor propagation model. Finally, numerical simulations have analyzed the possible influence factors on rumor propagation and proved the validity of the theoretical analysis.

Little attempt has been given on understanding and modeling rumor propagation in both temporal and spatial dimensions based on partial differential equation (PDE) models. How to define spatial distance is the key to solve PDE modeling. By using cluster importance as a distance, we abstractly translate the rumor propagation process in online social networks into two correlated processes: time growth process and space growth process, and then we establish a PDE mathematical model with a delay to describe rumor propagation. Theoretical analysis reveals the rich dynamic characteristics of rumor propagation, such as the local stability and the global stability. The numerical results describe the basic trend of rumor propagation in online social networks. This work is the first attempt to use partial differential equations to describe rumor spread on the basis of higher-order connectivity patterns.

I. INTRODUCTION

Rumor is a kind of general social phenomenon that public interested but improbable things, events, or unconfirmed interpretations of problems diffuse on a large scale in a short time through various means of communication among colleagues, friends, family members, and other people.[1] Different from the previous way of spreading a rumor by word of mouth, online social networks as an emerging network rumor transmission platform have been widely recognized and applied to spread rumors due to its flexibility, convenience, quickness, openness, and low cost. The interactivity of online social networks makes everyone be the rumor receivers and also the rumor disseminators. Thus, usually the number of rumor users increases by geometric series, and this kind of harm is difficult to measure. For example, a rumor, which comes from a web celebrity with thousands of fans, can be forwarded or commented to thousands of people in an instant, and even fission may be presented. As the prevailing of network rumor, research of rumor has become an urgent and serious theory topic with practical significance.

The spreading of rumor is in many ways similar to the spreading of epidemic infection, by the spreader or infectious to notify or infect the susceptible. After notified or infected, that the spreader can become the stifler is similar as the infectious can recover after a few time.[2] Mathematical model is an effective tool to analyze and predict both rumor propagation in online social networks and the spreading of infectious diseases among people. Recently, more and more scholars have started to study the problems of rumor spreading in online social networks based on epidemic models.[3–7,24,28] Zhao and Wang[8] established two rumor dynamical models with and without consideration of government measures, which contain four components: the susceptible individual, the spreader, the stifler, and the message in media. Stability was discussed in their work and the results showed that the amount of message released by government has the greatest influence on the rumor spread. Wang *et al.*[9] applied mean-field equations to describe the dynamics of a SIRaRu rumor spreading model in complex networks. Steady-state analysis of the SIRaRu model indicated that the threshold of rumor spreading existed in both homogeneous networks and inhomogeneous networks. Rumor propagation is often associated with the user's psychological activity. Zan *et al.*[10] had considered a self-resistance and counterattack mechanism in the process of rumor propagation in a new Susceptible-Infective-Counterattack-Refractory (SICR) model. The spreading peak of the rumor and the final state of the rumor were obtained in Ref. 10. Zhao *et al.*[11] had proposed that people had a variable forgetting rate in rumor propagation. Their analysis showed that the larger the initial forgetting rate or the faster the forgetting speed, the smaller the final size of the rumor spreading. Huo *et al.*[12] discussed the stability of the rumor-free equilibrium and the rumor-endemic equilibrium in a rumor transmission model with Holling-type II functional representing the scientific knowledge effect. This research provided the theoretical support to rumor control.

Most prior research studies in rumor propagation studied the characteristics of rumor propagation over various online social networks by using ordinary differential equation (ODE) models,[3–12] which only supposes rumor spreads along time orientation. As far as we know, little attempt has been given on understanding and modeling rumor propagation in both temporal and spatial dimensions based on PDE models. Wang *et al.*[13,14] previously proposed a PDE, specifically, a diffusive logistic equation to model the temporal and spatial characteristics of information diffusion. The data from Digg had verified the reliability of the PDE model. In Refs. 13 and 14, they used friendship hops to define a distance in the process of information diffusion. However, this kind of definition may only describe the spatial distance at $x = 1, 2, 3, \dots$, and this definition is invalid to some extent if $x = 0.5$ or $x = 1.5$. Our previous work[3,7] had also attempted to model rumor propagation over both temporal and spatial dimensions based on reaction-diffusion equations. We analyzed the stability, Hopf bifurcation of rumor spreading models and further showed how the rumor spreads in the spatial direction by the theorem of traveling wave solutions. However, Refs. 3 and 7 just stated the probability and the necessity of studying rumor temporal-spatial diffusion in online social networks by empiricism. For example, the development of mobile devices impelled rumor propagation over temporal and spatial dimensions.

In this paper, we use partial differential equations to study rumor spread in complex networks based on higher-order organizational structures. It is known that complex networks exhibit rich higher-order organizational structures that can be captured by clustering based on higher-order connectivity patterns.[15] Most of previous ODE or PDE modeling works are based on the lower-order connectivity. While lower-order connectivity patterns of complex networks can be captured at the level of individual nodes and edges; however, it remains largely unknown how higher-order organization of complex networks at the level of small network subgraphs affects information spread in complex networks. This work is the first attempt to use partial differential equations to describe information spread on the basis of higher-order connectivity patterns. Analysis of the PDE model reveals higher-order organization plays a significant role in information propagation in complex networks. This work can be applicable in information propagation units in neuronal networks and a hub structure in transportation networks.

In this paper, we define a novel abstract distance metric that is defined based on clustering techniques in Benson *et al.*[15] and clustering coefficients in graph theory. A abstract spatial distance metric in complex networks is critical to study rumor propagation over both temporal and spatial dimensions. The new distance metric effectively captures a key characteristic of information propagation in complex networks: information often spreads from one community to another. As a result of the new distance definition, we abstractly translate the rumor propagation process in online social networks into two correlated processes: time growth process and space growth process, and then we establish a PDE mathematical model with consideration of a latent delay during propagation to describe rumor diffusion over both temporal and spatial dimensions. Combined with the mathematical methods, we further study the stability of rumor equilibrium points, including the locally asymptotic stability and the globally asymptotic stability. Meanwhile, we will analyze the key factors that influence the spreading of rumors in online social networks by numerical simulations.

The remainder of this paper is organized as follows. In Sec. II, a modeling approach is described explicitly. In Sec. III, *a priori* bound of the solution and the existence of equilibrium points are established. In Sec. IV, we study the stability of our proposed model. In Sec. V, to support our theoretical predictions, some numerical simulations are given. Finally, a brief summary is given to finish this work.

II. MODELING RUMOR PROPAGATION OVER BOTH TEMPORAL AND SPATIAL DIMENSIONS

An online social network is a social structure made of nodes (individuals or organizations) and edges that connect nodes if the nodes are related by the relationship that characterizes the network, for example, friendship, colleagueship, and so on. Therefore, social networks can be reasonably modeled by graphs, which we often consider a closed and mixed population consisting of N individuals as a complex network. As graphs, online social networks often exhibit a community structure with inherent clusters. Clustering is important for modeling rumor propagation in online social networks as clustering usually can be used to define distance in social media. This distance captures the natural characteristic of rumor propagation processes from one cluster to another. Detecting clusters is one of the critical tasks in social network analysis due to its broad applications such as friend recommendations, link predictions, and collaborative filtering. Moreover, the in-depth understanding of the structure of cluster in social networks could also dissect the characterizations and modeling of rumor propagation in both temporal and spatial dimensions over online social networks.

Recently, Benson *et al.*[15] point out that higher-order connectivity patterns are essential to understanding the fundamental network structures. The most common higher-order structures are small network subgraphs, which is referred to as network motifs in Ref. 15 [see Fig. 1(A) in Ref. 15] and the triangular motif can be considered building blocks for online social networks. We use the concept of network motifs proposed by Benson to search for clusters of an online social network. Because a social network usually contains tens of thousands of user nodes, it is inconvenient for us to give a community detection according to a social network in the current work. Thus, in the next, for the sake of simplicity we will take a simple network to introduce our method for searching for clusters, which is important for us to describe rumor propagation in both temporal and spatial dimensions based on a PDE mathematical model.

Definition 1 (Ref. 15). Given an unweighted, directed graph and a motif set M, define the motif adjacency matrix by

$$(W_M)_{ij} = \text{number of motif instances in } M \text{ where } i \text{ and } j \text{ participate in the motif.} \tag{1}$$

Then, accordingly we can define the motif diagonal degree matrix by $(D_M)_{ij} = \sum_{j=1}^{n}(W_M)_{ij}$ and the motif Laplacian as $L_M = D_M - W_M$.

In this work, graph partition aims to find out a partition such that the cut (the total number of motif instances cut) is minimized. Two commonly used variants are *ratio cut* and *normalized cut*. Consider a graph $G = (V, E)$. Let $\zeta = (S_1, S_2, \ldots, S_k)$ be a graph partition such that $S_i \cap S_j = \varnothing$ and $\cup_{i=1}^{k} S_i = V$. The ratio cut and the normalized cut are defined as

$$\text{Ratio cut}(\zeta) = \frac{1}{k}\sum_{i=1}^{k}\frac{cut(S_i, \overline{S}_i)}{|S_i|}, \tag{2}$$

$$\text{Normalized cut}(\zeta) = \frac{1}{k}\sum_{i=1}^{k}\frac{cut(S_i, \overline{S}_i)}{vol(S_i)}, \tag{3}$$

where $\overline{S}_i$ denotes the remainder of the nodes (the complement of S_i), $cut(S_i, \overline{S}_i)$ is the number of instances of motif M with at least one node in S_i and one in $\overline{S}_i$, and $vol(S_i)$ is the number of nodes in instances of M that reside in S_i.

Nevertheless, finding the minimum ratio cut or normalized cut is NP-hard. A good way to solve this problem is to transform the original optimal partition problem of graph into a continuous and relaxed form and then to solve a spectral factorization problem of some spectral clustering matrix.[16] Spectral clustering[16] is an effective method, which is derived from the problem of graph partition, since we want to search for clusters.

Based on the above preparations, now we consider a simple network graph, which comes from Fig. 1(C) in Ref. 15, as an example to search for clusters.

For the given graph and a motif of interest (in this case, M_7 is selected in Ref. 15), we can compute the corresponding motif Laplacian

$$L_M = D_M - W_M = \begin{pmatrix} 6 & -3 & -1 & -1 & -1 & 0 & 0 & 0 & 0 & 0 \\ -3 & 8 & -1 & -1 & -1 & -1 & -1 & 0 & 0 & 0 \\ -1 & -1 & 2 & 0 & 0 & 0 & 0 & 0 & 0 & 0 \\ -1 & -1 & 0 & 2 & 0 & 0 & 0 & 0 & 0 & 0 \\ -1 & -1 & 0 & 0 & 2 & 0 & 0 & 0 & 0 & 0 \\ 0 & -1 & 0 & 0 & 0 & 4 & -1 & -1 & -1 & 0 \\ 0 & -1 & 0 & 0 & 0 & -1 & 2 & 0 & 0 & 0 \\ 0 & 0 & 0 & 0 & 0 & -1 & 0 & 4 & -2 & -1 \\ 0 & 0 & 0 & 0 & 0 & -1 & 0 & -2 & 4 & -1 \\ 0 & 0 & 0 & 0 & 0 & 0 & 0 & -1 & -1 & 2 \end{pmatrix}. \tag{4}$$

Then, the eigenvalue λ_i $(i = 1, 2, \ldots, 10)$ and the eigenvector z_i $(i = 1, 2, \ldots, 10)$ of the Laplacian transformation of the motif adjacency matrix L_M are computed as

$$\lambda_1 = 0, \quad \lambda_2 = 0.3846, \quad \lambda_3 = 1.5957, \quad \lambda_{4,5} = 2.0000, \quad \lambda_6 = 3.0000,$$
$$\lambda_7 = 5.0000, \quad \lambda_8 = 5.6657, \quad \lambda_9 = 6.0000, \quad \lambda_{10} = 10.3540$$

and

$$z_1 = (0.3162\ \ 0.3162\ \ 0.3162\ \ 0.3162\ \ 0.3162\ \ 0.3162\ \ 0.3162\ \ 0.3162\ \ 0.3162\ \ 0.3162)^T,$$

$$z_2 = (-0.2788\ \ -0.2157\ \ -0.3061\ \ -0.3061\ \ -0.3061\ \ 0.1516\ \ -0.0397\ \ 0.4017\ \ 0.4017\ \ 0.4974)^T,$$

$$z_3 = (0.1104\ \ -0.0319\ \ 0.1939\ \ 0.1939\ \ 0.1939\ \ -0.2990\ \ -0.8185\ \ 0.0658\ \ 0.0658\ \ 0.3256)^T,$$

$$z_4 = (0.0000\ \ -0.0000\ \ 0.0451\ \ 0.6835\ \ -0.7285\ \ -0.0000\ \ -0.0000\ \ -0.0000\ \ 0.0000\ \ 0.0000)^T,$$

$$z_5 = (0.0000\ \ 0.0000\ \ -0.8153\ \ 0.4466\ \ 0.3686\ \ 0.0000\ \ -0.0000\ \ 0.0000\ \ -0.0000\ \ 0.0000)^T,$$

$$z_6 = (0.0000\ \ 0.0000\ \ 0.0000\ \ -0.0000\ \ 0.0000\ \ -0.3536\ \ 0.3536\ \ -0.3536\ \ -0.3536\ \ 0.7071)^T,$$

$$z_7 = (0.2070\ \ 0.2070\ \ -0.1380\ \ -0.1380\ \ -0.1380\ \ 0.7246\ \ -0.3105\ \ -0.3105\ \ -0.3105\ \ 0.2070)^T,$$

$$z_8 = (-0.6862 \quad -0.3626 \quad 0.2861 \quad 0.2861 \quad 0.2861 \quad 0.3507 \quad 0.0032 \quad -0.1124 \quad -0.1124 \quad 0.0613)^T,$$

$$z_9 = (-0.0000 \quad 0.0000 \quad 0.0000 \quad 0.0000 \quad -0.0000 \quad 0.0000 \quad 0.0000 \quad 0.7071 \quad -0.7071 \quad -0.0000)^T,$$

$$z_{10} = (0.5444 \quad -0.8235 \quad 0.0334 \quad 0.0334 \quad 0.0334 \quad 0.1211 \quad 0.0841 \quad -0.0149 \quad -0.0149 \quad 0.0036)^T.$$

In this graph, we aim to cluster a network into three clusters based on motif M_7. In Ref. 15, for clustering a network into more than two clusters based on motifs, the authors had provided their own approach as recursive bi-partitioning. The core idea of this approach is to continue to cut the largest remaining cluster until the network is partitioned into some pre-specified number of clusters. This approach will eventually run **k**-means clustering algorithm partitions, and it could ensure the reliability of the results. Thus, in the following, we will apply **k**-means to solve our problem in our way. Typically, the first eigenvector does not contain any community information.[17] Thus, we only need to consider eigenvectors z_2 and z_3 to run the **k**-means algorithm on the 2-dimensional data. Now, we can give the following data set:

$$X = \left[\begin{array}{c|cc} & X_1 & X_2 \\ 1 & -0.2788 & 0.1104 \\ 2 & -0.2157 & -0.0319 \\ 3 & -0.3061 & 0.1939 \\ 4 & -0.3061 & 0.1939 \\ 5 & -0.3061 & 0.1939 \\ 6 & 0.1516 & -0.2990 \\ 7 & -0.0397 & -0.8185 \\ 8 & 0.4017 & 0.0658 \\ 9 & 0.4017 & 0.0658 \\ 10 & 0.4974 & 0.3256 \end{array}\right],$$

where each column above indicates one attribute (X_1 and X_2, respectively).

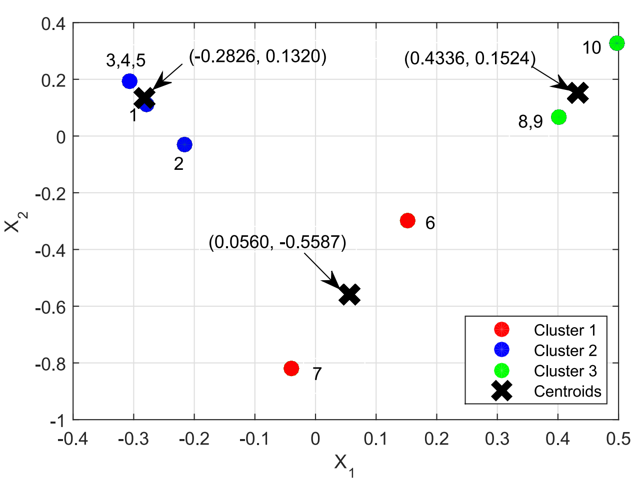

FIG. 1. Cluster assignment and corresponding centroids.

For the given parameter $\mathbf{k} = 3$ in this section, the **k**-means clustering algorithm partitions data instances in set X into three clusters. Each cluster is associated with a centroid. In Fig. 1, we show the three centroids as $(0.0560, -0.5587)$, $(-0.2826, 0.1320)$, and $(0.4336, 0.1524)$. The centroid of a cluster is typically computed as the mean of the data points assigned to the cluster. Each data point is assigned to the closest cluster, or the distance between its centroid and the data point is the shortest. We here employ the Euclidean distance to compute the minimum distance between the data point and the centroid as Table I shows. In Fig. 1, the centroids do not change anymore, and the **k**-means clustering algorithm converges. Thus, we can obtain three clusters as $\{1, 2, 3, 4, 5\}$, $\{6, 7\}$, and $\{8, 9, 10\}$.

So far, we have successfully clustered a network in Ref. 15 into three clusters based on motif M_7. However, in order to define a reasonable spatial distance for rumor propagation in online social networks, we must analyze the importance between the different clusters in the next. To do this, we must first discuss the node importance measurement. As we all know it, the single indicator to measure the importance of the network nodes will lose more node information and it is short of accuracy. Recently, combined with some important factors, such as the degree of centrality, the relative closeness centrality, clustering coefficient, and so on, Wang[26] provided an integrated measuring method to measure the nodes' importance. Moreover, Hu and Mei[27] had raised a novel ranking method of influential nodes using structural holes called the E-Burt method, which was suitable for the weighted networks. In this paper, based on the degree and clustering coefficient information,[18] we will rank the importance of the nodes. Usually, the degree can only give priority to the neighbor size, regardless of the clustering property of the neighbors. The clustering coefficient just only measures the closeness among the neighbors and neglects the activity of the target node. Thus, combining neighbor and clustering coefficient information can achieve a more comprehensive evaluation.[18]

TABLE I. Euclidean distance between the data point and the centroid.

	Centroid 1	Centroid 2	Centroid 3
Node 1	0.5598	0.0005	0.5093
Node 2	0.3514	0.0313	0.4556
Node 3	0.6976	0.0044	0.5489
Node 4	0.6976	0.0044	0.5489
Node 5	0.6976	0.0044	0.5489
Node 6	0.0766	0.3743	0.2833
Node 7	0.0766	0.9625	1.1667
Node 8	0.5096	0.4726	0.0085
Node 9	0.5096	0.4726	0.0085
Node 10	0.9770	0.6458	0.0341

For a given directed graph G without consideration of self-interactions, the degree of the node usually has three components: the number of outgoing links $k_i^{out} = \sum_j \delta_{ij}$ (referred to as the out-degree of the node), the number of ingoing links $k_i^{in} = \sum_j \delta_{ji}$ (referred to as the in-degree of the node), and the number of bilateral edges between i and its neighbors $k_i^{\leftrightarrow} = \sum_{j\neq i} \delta_{ij}\delta_{ji}$ (i.e., the number of nodes j for which both an edge $i \to j$ and an edge $j \to i$ exist). The total degree is then defined as

$$k_i = k_i^{out} + k_i^{in} - k_i^{\leftrightarrow}, \tag{5}$$

where $\delta_{ij} = 1$ if and only if there is an edge $i \to j$ (i.e., if they are neighbors) and zero otherwise.

The clustering coefficient for node i (c_i) in the above directed graph G can be defined as the ratio between all directed triangles actually formed by i (t_i) and the number of all possible triangles that i could form (T_i).[19] Thus, we obtain

$$c_i = \frac{t_i}{T_i} = \frac{\sum_j \sum_h (\delta_{ij} + \delta_{ji})(\delta_{ih} + \delta_{hi})(\delta_{jh} + \delta_{hj})}{2[(k_i + k_i^{\leftrightarrow})(k_i + k_i^{\leftrightarrow} - 1) - 2k_i^{\leftrightarrow}]}. \tag{6}$$

Recently, Ren *et al.*[18] put forward a new node importance evaluation index p_i in networks by combining the neighbor node information and the cluster coefficient. p_i is defined as

$$p_i = \frac{f_i}{\sqrt{\sum_{j=1}^N f_j^2}} + \frac{g_i}{\sqrt{\sum_{j=1}^N g_j^2}}, \tag{7}$$

where

$$f_i = k_i + \sum_{\chi \in \Gamma_i} k_\chi, \tag{8}$$

$$g_i = \frac{\max_{j=1}^N \left\{\frac{c_j}{f_j}\right\} - \frac{c_i}{f_i}}{\max_{j=1}^N \left\{\frac{c_j}{f_j}\right\} - \min_{j=1}^N \left\{\frac{c_j}{f_j}\right\}}, \tag{9}$$

where N is the number of the nodes in G, k_χ is the degree of node χ, Γ_i is the set of the neighbour nodes of node i, and c_i is the clustering coefficient. Obviously, f_i reflects the degree information of node itself and its neighbors' nodes, and g_i reflects the closeness of its neighbor nodes.

Now, according to Eqs. (5)–(9), we can establish the node attributes by a direct calculation as shown in Table II. In order to evaluate and compare the three clusters $\{1, 2, 3, 4, 5\}$, $\{6, 7\}$, and $\{8, 9, 10\}$, we further calculate an average node importance evaluation index of each cluster based on p_i in Table II. In cluster $\{1, 2, 3, 4, 5\}$, we define an average node importance evaluation index $P_1 = \frac{p_1+p_2+p_3+p_4+p_5}{5}$. Similarly, we have $P_2 = \frac{p_6+p_7}{2}$ in cluster $\{6, 7\}$ and $P_3 = \frac{p_8+p_9+p_{10}}{3}$ in cluster $\{8, 9, 10\}$. A direct calculation shows $P_1 = 0.5433$, $P_2 = 0.7540$, and $P_3 = 0.5205$. Clearly, $P_2 > P_1 > P_3$. Thus, we can say that the importance of the three clusters in turn order is $\{6, 7\}$, $\{1, 2, 3, 4, 5\}$, and $\{8, 9, 10\}$. In fact, the result can be accepted intuitively from Table II. Through comparative analysis of index p_i, we find that the importance of nodes 3, 4, 5, and 10 is relatively lower. Moreover, nodes 3, 4, 5, and 10 have the least amount of neighbor nodes, and the degree of closeness between their neighbor nodes is also lower, which can be found from the value of g_i. These phenomena comprehensively show that nodes 3, 4, 5, and 10 will lessen the importance of cluster $\{1, 2, 3, 4, 5\}$ and $\{8, 9, 10\}$, even though there exist some important nodes in the two clusters, respectively.

TABLE II. Node attributes of a network in Fig. 2.

Node	k_i	f_i	c_i	g_i	p_i
1	5	23	0.2857	0.9396	0.7638
2	7	30	0.2037	1.0000	0.8995
3	2	14	1.0000	0.3065	0.3510
4	2	14	1.0000	0.3065	0.3510
5	2	14	1.0000	0.3065	0.3510
6	5	28	0.3214	0.9497	0.8466
7	3	19	0.4000	0.8470	0.6614
8	4	22	0.2778	0.9374	0.7472
9	4	18	0.3333	0.8742	0.6574
10	2	10	1.0000	0.0000	0.1567

In the following, according to the importance of clusters we have obtained, we can model rumor propagation in both temporal and spatial dimensions. We are interested in answering the "spatio-temporal propagation problem": how to define the spatial distance of rumor propagation? For an initial rumor (define it as a *source*) in online social networks, after a time period t, what is the density of influenced users at distance x from the *source*? Here, we use "cluster importance" as a distance. For example, because there exist three different clusters according to the above analysis, we define the maximum distance of rumor propagation as 3 and in turn define the location of each cluster as $x \in [0, 1)$ for cluster 1 ($\{6, 7\}$), $x \in [1, 2)$ for cluster 2 ($\{1, 2, 3, 4, 5\}$), and $x \in [2, 3]$ for cluster 3 ($\{8, 9, 10\}$) by their importance (as shown in Fig. 2). Further, we abstractly translate the rumor propagation process in online social networks into two correlated processes: time growth process and space growth process. The time growth process represents rumor spreads among users over time flying at an arbitrary given distance of each cluster, and the space growth process is the process through which rumor randomly diffuses among users at different distances from the source, that is to say, rumor may diffuse among the same cluster or between different clusters in this process.

As is known to all, mathematical modeling is an effective approach in extracting the nature of rumor propagation in online social networks. How to reflect the above two process of rumor propagation in a mathematical modeling is challenging. PDE, which is combined with time scale and space scale, effectively describes the space-time developing rules of all things. PDE has been widely used in the study of infectious diseases, hydromechanics, chemistry, and so on. Thus, since we have defined the spatial distance of rumor propagation by *cluster importance*, the PDE mathematical model becomes our first choice to reflect rumor spatio-temporal diffusion according to our proposed diffusion form.

Thus far, we have discussed and solved the problem of how to model rumor spatio-temporal diffusion based on a simple network in Ref. 15. Usually, a real online social network consists tens of thousands of nodes. Reference 15 found that in real online social networks, there really existed a motif-based cluster by selecting a complete 2010 Twitter follower graph (the graph consists of 41.65 million nodes and 1.47 billion edges) to analyze clusters. For a given online

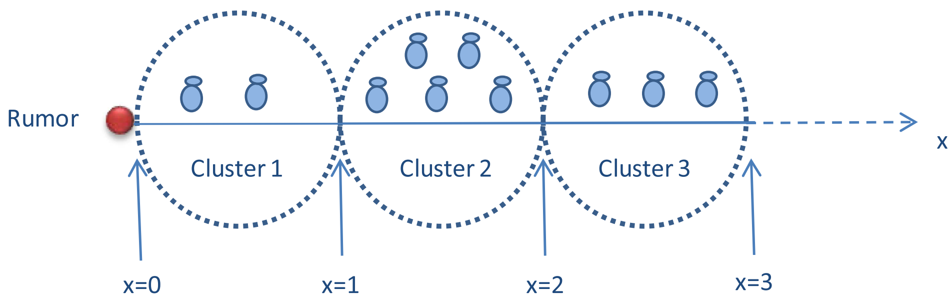

FIG. 2. Rumor propagation processes in online social networks.

social network, we can use the same method as we have provided in the above to model rumor spatio-temporal diffusion. Because the number of nodes in a real online social network is very large, considering an online social network being separated into L clusters is more appropriate. That is to say, the furthest distance of rumor propagation is L. In the following, based on the classical epidemic model and combined with the idea of defining *cluster importance* as a distance, we propose a PDE rumor propagation model in online social networks.

Generally, the users in an online social network can be divided into three classes depending on their different states: *susceptible user* (i.e., a user who lacks social and self-protection awareness may be infected by the rumor propagation), *infected user* (i.e., a user is infected by rumor, meaning that the user may infect his neighbors by diffusing the rumor, but the rumor has not been initiated by the user), and *recovered user* (i.e., a user no longer believes the rumor and the rumor stops diffusion among this type of users). For simplicity, similar to epidemic models,[21–23] we use $S(t,x)$, $I(t,x)$, and $R(t,x)$ to represent the densities of susceptible users, infected users, and recovered users with a distance of x at time t, respectively.

To model the propagation of rumor in online social networks, the following assumptions are imposed:

(i) Social network is an open network, which implies that users are free to enter or exit the social network by some ratio.
(ii) Rumor propagation between susceptible users and infected user submits to the saturated incidence rate and in this process there exists a time delay, which can be seen as a latent period. Meanwhile, further considering the exit rate factor for the latent period is also significant.
(iii) Usually, recovered users can affect infected users by clarifying the truth of the rumor such that infected users become recovered users. This process may be described by a bilinear incidence rate between infected users and recovered users.

From the above assumptions and descriptions, our model can be represented as a set of coupled partial functional differential equations as follows:

$$\begin{cases} \dfrac{\partial S(t,x)}{\partial t} = d\Delta S(t,x) + \mu - \dfrac{\beta_1 S(t,x)I(t,x)}{1+\alpha I(t,x)} - \mu S(t,x), \\ \dfrac{\partial I(t,x)}{\partial t} = d\Delta I(t,x) + \dfrac{\beta_1 S(t-\tau,x)I(t-\tau,x)}{1+\alpha I(t-\tau,x)} e^{-\mu\tau} - \beta_2 I(t,x)R(t,x) - \mu I(t,x), \\ \dfrac{\partial R(t,x)}{\partial t} = d\Delta R(t,x) + \beta_2 I(t,x)R(t,x) - \mu R(t,x), \end{cases} \tag{10}$$

for $t>0$, $x \in \Omega$ with homogeneous Neumann boundary conditions

$$\frac{\partial S}{\partial n}(t,x) = \frac{\partial I}{\partial n}(t,x) = \frac{\partial R}{\partial n}(t,x) = 0, \quad t \geq 0,\ x \in \partial\Omega, \tag{11}$$

and initial conditions

$$\begin{cases} S(t,x) = S_0(t,x) \geq 0 \quad \text{and} \not\equiv 0,\ (t,x) \in [-\tau,0]\times\bar{\Omega}, \\ I(t,x) = I_0(t,x) \geq 0 \quad \text{and} \not\equiv 0,\ (t,x) \in [-\tau,0]\times\bar{\Omega}, \\ R(t,x) = R_0(t,x) \geq 0 \quad \text{and} \not\equiv 0,\ (t,x) \in [-\tau,0]\times\bar{\Omega}, \end{cases} \tag{12}$$

where d, μ, β_1, β_2, α, and τ are all positive constants. d is the diffusion coefficient, μ is the entry and exit rate, β_1 is the rumor transmission rate, β_2 is the recovery rate of infected users, α describes the psychological effect of infected users in the process of rumor propagation, τ accounts for the time delay (we can also define it as a latent period) between infected users transmits a rumor to susceptible users and the production of newly infected users. $\Omega = [0,L]$ is the bounded domain with smooth boundary $\partial\Omega$ and L is the maximum distance of space. $\Delta = \partial^2/\partial x^2$ is a Laplace operator. $\frac{\beta_1 SI}{1+\alpha I}$ is a saturated incidence rate presenting rumor diffusion between susceptible users and infected users. $\beta_2 IR$ is the bilinear incidence rate presenting infected users becoming recovered users. The exit rate factor for the latent period is described by $e^{-\mu\tau}$. The boundary condition in (11) implies that there are no rumors across the boundary of Ω. $S_0(t,x)$, $I_0(t,x)$, and $R_0(t,x)$, as the initial density functions are non-negative, Hölder continuous, and satisfy $\partial S_0(t,x)/\partial n = 0$, $\partial I_0(t,x)/\partial n = 0$, and $\partial R_0(t,x)/\partial n = 0$ on $[-\tau,0]\times\partial\Omega$.

III. WELL-POSEDNESS AND EXISTENCE OF EQUILIBRIUM POINTS

In this section, the existence of solution to the dynamical equations (10)–(12) is proved, and *a priori* bound of the solution is also established. Meanwhile, we analyze the existence of equilibrium points under some necessary assumptions.[29,35–39]

Theorem 1. Let $(S(t,x), I(t,x), R(t,x))$ be a solution of system (10) with homogeneous Neumann boundary conditions (11) and initial conditions (12). Then, $(S(t,x), I(t,x), R(t,x))$ is non-negative and uniformly bounded for any $t > 0$ and $x \in \Omega$. More precisely, we have

$$\limsup_{t\to+\infty, x\in\Omega} (S(t,x), I(t,x), R(t,x)) \le e^{-\mu\tau}(e^{\mu\tau}, 1, 1). \tag{13}$$

Proof. Define

$$\begin{aligned}
H(S(t,x), I(t,x), R(t,x)) &= \mu - \frac{\beta_1 S(t,x)I(t,x)}{1+\alpha I(t,x)} - \mu S(t,x),\\
M(S(t,x), I(t,x), R(t,x)) &= \frac{\beta_1 S(t-\tau,x)I(t-\tau,x)}{1+\alpha I(t-\tau,x)}e^{-\mu\tau}\\
&\quad - \beta_2 I(t,x)R(t,x) - \mu I(t,x),\\
N(S(t,x), I(t,x), R(t,x)) &= \beta_2 I(t,x)R(t,x) - \mu R(t,x).
\end{aligned}$$

A direct calculation shows that the dynamical equation (10) is a mixed quasimonotone system. Now, let $(\underline{S}(t,x), \underline{I}(t,x), \underline{R}(t,x)) = (0,0,0)$ and $(\overline{S}(t,x), \overline{I}(t,x), \overline{R}(t,x)) = (S^*(t), I^*(t), R^*(t))$, where $(S^*(t), I^*(t), R^*(t))$ is the unique solution to

$$\begin{cases}
\dfrac{dS(t)}{dt} = \mu - \mu S(t),\\[2mm]
\dfrac{dI(t)}{dt} = \dfrac{\beta_1 S(t-\tau)I(t-\tau)}{1+\alpha I(t-\tau)}e^{-\mu\tau} - \mu I(t),\\[2mm]
\dfrac{dR(t)}{dt} = \beta_2 I(t)R(t) - \mu R(t),
\end{cases} \tag{14}$$

with initial conditions

$$\begin{cases}
S(t) = S_0^*(t) \ge 0, & t \in [-\tau, 0],\\
I(t) = I_0^*(t) \ge 0, & t \in [-\tau, 0],\\
R(t) = R_0^*(t) \ge 0, & t \in [-\tau, 0],
\end{cases} \tag{15}$$

where $S_0^*(t) = \sup_{x\in\overline{\Omega}} S_0(t,x)$, $I_0^*(t) = \sup_{x\in\overline{\Omega}} I_0(t,x)$, $R_0^*(t) = \sup_{x\in\overline{\Omega}} R_0(t,x)$.

Obviously, it is easy to see that for any initial conditions satisfying (15), we have

$$\mu - \mu S(t)|_{S(t)=0} \ge 0, \quad \left.\frac{\beta_1 S(t-\tau)I(t-\tau)}{1+\alpha I(t-\tau)}e^{-\mu\tau} - \mu I(t)\right|_{I(t)=0} \ge 0$$

and

$$\beta_2 I(t)R(t) - \mu R(t)|_{R(t)=0} \ge 0.$$

Thus, according to Refs. 20 and 25, we obtain $S^*(t) \ge 0$, $I^*(t) \ge 0$, and $R^*(t) \ge 0$. Then $(\underline{S}(t,x), \underline{I}(t,x), \underline{R}(t,x)) = (0,0,0)$ and $(\overline{S}(t,x), \overline{I}(t,x), \overline{R}(t,x)) = (S^*(t), I^*(t), R^*(t))$ are the lower-solution and upper-solution to system (10), respectively, since

$$\begin{aligned}
&\frac{\partial \overline{S}(t,x)}{\partial t} - d\Delta\overline{S}(t,x) - H(\overline{S}(t,x), \underline{I}(t,x)) = 0 \ge 0,\\
&\frac{\partial \underline{S}(t,x)}{\partial t} - d\Delta\underline{S}(t,x) - H(\underline{S}(t,x), \overline{I}(t,x)) = -\mu \le 0,\\
&\frac{\partial \overline{I}(t,x)}{\partial t} - d\Delta\overline{I}(t,x) - M(\overline{S}(t,x), \overline{I}(t,x), \underline{R}(t,x)) = 0 \ge 0\\
&\quad = \frac{\partial \underline{I}(t,x)}{\partial t} - d\Delta\underline{I}(t,x) - M(\underline{S}(t,x), \underline{I}(t,x), \overline{R}(t,x)),
\end{aligned}$$

and

$$\begin{aligned}
&\frac{\partial \overline{R}(t,x)}{\partial t} - d\Delta\overline{R}(t,x) - N(\overline{I}(t,x), \overline{R}(t,x))\\
&\quad = 0 \ge 0 = \frac{\partial \underline{R}(t,x)}{\partial t} - d\Delta\underline{R}(t,x) - N(\underline{I}(t,x), \underline{R}(t,x)),
\end{aligned}$$

the homogeneous Neumann boundary conditions are satisfied, and $0 \le S_0(t,x) \le S_0^*(t)$, $0 \le I_0(t,x) \le I_0^*(t)$, and $0 \le R_0(t,x) \le R_0^*(t)$ for any $t \in [-\tau, 0]$, $x \in \overline{\Omega}$.

Therefore, system (10) has a unique globally defined solution $(S(t,x), I(t,x), R(t,x))$ which satisfies

$$\begin{aligned}
&0 \le S(t,x) \le S^*(t), \quad 0 \le I(t,x) \le I^*(t),\\
&0 \le R(t,x) \le R^*(t), \quad t \ge 0.
\end{aligned}$$

Further, in order to prove the uniform boundedness of solution and obtain (13), we define

$$G(t,x) = e^{-\mu\tau}S(t,x) + I(t+\tau,x) + R(t+\tau,x). \tag{16}$$

Differentiating $G(t,x)$ with respect to time t along the solution of (10) yields

$$\begin{aligned}
\left.\frac{\partial G(t,x)}{\partial t}\right|_{(10)} &= e^{-\mu\tau}\left(d\frac{\partial^2 S(t,x)}{\partial x^2} + \mu - \frac{\beta_1 S(t,x)I(t,x)}{1+\alpha I(t,x)} - \mu S(t,x)\right)\\
&\quad + d\frac{\partial^2 I(t+\tau,x)}{\partial x^2} + \frac{\beta_1 S(t,x)I(t,x)}{1+\alpha I(t,x)}e^{-\mu\tau}\\
&\quad - \beta_2 I(t+\tau,x)R(t+\tau,x) - \mu I(t+\tau,x)\\
&\quad + d\frac{\partial^2 R(t+\tau,x)}{\partial x^2} + \beta_2 I(t+\tau,x)R(t+\tau,x)\\
&\quad - \mu R(t+\tau,x)\\
&= d\frac{\partial^2}{\partial x^2}\left(e^{-\mu\tau}S(t,x) + I(t+\tau,x) + R(t+\tau,x)\right)\\
&\quad + \mu e^{-\mu\tau} - \mu\left(e^{-\mu\tau}S(t,x) + I(t+\tau,x) + R(t+\tau,x)\right)\\
&= d\frac{\partial^2 G(t,x)}{\partial x^2} + \mu e^{-\mu\tau} - \mu G(t,x).
\end{aligned}$$

Then, we have

$$\limsup_{t\to+\infty, x\in\Omega} G(t,x) = e^{-\mu\tau}.$$

On the other hand, it has been proved that $S(t,x)$, $I(t,x)$, and $R(t,x)$ are non-negative. Thus, according to Eq. (16) for any $t \ge -\tau$, we have

$e^{-\mu\tau}S(t,x) \le G(t,x)$, which implies that

$$\limsup_{t\to+\infty, x\in\Omega} S(t,x) \le \limsup_{t\to+\infty, x\in\Omega} e^{\mu\tau}G(t,x) = 1.$$

Using the similar argument for $I(t,x)$ and $R(t,x)$, we can obtain the result listed in (13). □

Theorem 2. System (10) has an infection-free equilibrium point $E_0 = (1,0,0)$, corresponding to the maximal level of susceptible users. This is the only meaningful equilibrium point in network informatics if

$$\mathscr{R}_0 = \frac{\beta_1}{\mu}e^{-\mu\tau} < 1. \tag{17}$$

If $\mathscr{R}_0 > 1$, in addition to E_0, there exists another meaningful equilibrium point in network informatics,

$$\begin{aligned} E_1 &= \left(\frac{\mu\alpha+\mu e^{\mu\tau}}{\beta_1+\mu\alpha}, \frac{-\mu+\beta_1 e^{-\mu\tau}}{\beta_1+\mu\alpha}, 0\right) \\ &= \left(\frac{\mu\alpha+\mu e^{\mu\tau}}{\beta_1+\mu\alpha}, \frac{\mu(\mathscr{R}_0-1)}{\beta_1+\mu\alpha}, 0\right), \end{aligned}$$

which corresponds to positive levels of susceptible users and infected users, but no recovered users. If

$$\mathscr{R}_1 = \frac{\beta_1\beta_2}{\mu(\beta_1+\beta_2+\mu\alpha)}e^{-\mu\tau} > 1, \tag{18}$$

or equivalently

$$\mathscr{R}_0 > 1 + \frac{\beta_1+\mu\alpha}{\beta_2}, \tag{19}$$

system (10) also has an interior equilibrium point

$$\begin{aligned} E_2 &= \left(\frac{\beta_2+\mu\alpha}{\beta_1+\beta_2+\mu\alpha}, \frac{\mu}{\beta_2}, \frac{\beta_1\beta_2 e^{-\mu\tau}-\mu(\beta_1+\beta_2+\mu\alpha)}{\beta_2(\beta_1+\beta_2+\mu\alpha)}\right) \\ &= \left(\frac{\beta_2+\mu\alpha}{\beta_1+\beta_2+\mu\alpha}, \frac{\mu}{\beta_2}, \frac{\mu(\beta_1+\beta_2+\mu\alpha)(\mathscr{R}_1-1)}{\beta_2(\beta_1+\beta_2+\mu\alpha)}\right), \end{aligned}$$

accounting for the presence of all three components: susceptible users, infected users, and recovered users.

Remark 1. In fact

$$\mathscr{R}_1 = \frac{\beta_2}{\beta_1+\beta_2+\mu\alpha}\cdot\mathscr{R}_0 < \mathscr{R}_0.$$

Thus, we have the following:

(i) if $\mathscr{R}_0 < 1$, then there is only one equilibrium point E_0;
(ii) if $\mathscr{R}_0 > 1$ and $\mathscr{R}_1 \le 1$, then there are two equilibrium points E_0 and E_1;
(iii) if $\mathscr{R}_1 > 1$, then there are three equilibrium points E_0, E_1, and E_2.

IV. STABILITY ANALYSIS OF EQUILIBRIUM POINTS

In this section, we will discuss the locally asymptotic stability and the globally asymptotic stability of equilibrium points E_0, E_1, and E_2 by the linearization technique and the Lyapunov function method.[30–34]

We introduce a phase space $\mathscr{C} = C([-\tau,0],X)$, where $X = \{u \in W^{2,2}(\Omega);\ \frac{\partial u}{\partial n} = 0 \text{ on } \partial\Omega\}$ with the inner product $\langle\cdot,\cdot\rangle$. Without loss of generality, let $\tilde{S} = S - S^\star$, $\tilde{I} = I - I^\star$, $\tilde{R} = R - R^\star$, where $(S^\star, I^\star, R^\star)$ is an arbitrary equilibrium point of system (10), and then drop bars for the simplicity of notations. Therefore, system (10) can be transformed into the following form:

$$\begin{cases} \dfrac{\partial S(t,x)}{\partial t} = d\Delta S(t,x) - \left(\mu + \dfrac{\beta_1 I^\star}{1+\alpha I^\star}\right)S(t,x) - \dfrac{\beta_1 S^\star}{(1+\alpha I^\star)^2}I(t,x) + \displaystyle\sum_{i+j\ge 2}\frac{1}{i!j!}H_{ij}S^i(t,x)I^j(t,x), \\ \dfrac{\partial I(t,x)}{\partial t} = d\Delta I(t,x) + \dfrac{\beta_1 I^\star}{1+\alpha I^\star}e^{-\mu\tau}S(t-\tau,x) - (\beta_2 R^\star + \mu)I(t,x) + \dfrac{\beta_1 S^\star}{(1+\alpha I^\star)^2}e^{-\mu\tau}I(t-\tau,x) \\ \qquad -\beta_2 I^\star R(t,x) + \displaystyle\sum_{h+i+j+l\ge 2}\frac{1}{h!i!j!l!}M_{hijl}S^h(t-\tau,x)I^i(t,x)I^j(t-\tau,x)R^l(t,x), \\ \dfrac{\partial R(t,x)}{\partial t} = d\Delta R(t,x) + \beta_2 R^\star I(t,x) + (\beta_2 I^\star - \mu)R(t,x) + \displaystyle\sum_{i+j\ge 2}\frac{1}{i!j!}N_{ij}I^i(t,x)R^j(t,x), \end{cases} \tag{20}$$

where

$$\begin{aligned} H_{ij} &= \frac{\partial^{i+j}H}{\partial^i S(t,x)\partial^j I(t,x)}, \\ M_{hijl} &= \frac{\partial^{h+i+j+l}M}{\partial^h S(t-\tau,x)\partial^i I(t,x)\partial^j I(t-\tau,x)\partial^l R(t,x)}, \\ N_{ij} &= \frac{\partial^{i+j}N}{\partial^i I(t,x)\partial^j R(t,x)}. \end{aligned}$$

Thus, the equilibrium point $(S^\star, I^\star, Y^\star)$ of system (10) is transformed into the zero equilibrium point $(0,0,0)$ of system (20).

In the following, in order to analyze the locally asymptotic stability of E_0, E_1, and E_2 of system (10), we can discuss the stability of the equilibrium point $(0,0,0)$ of system (20).

Denote

$$U(t) = (u_1(t), u_2(t), u_3(t))^T = (S(t,\cdot), I(t,\cdot), R(t,\cdot))^T,$$

then system (20) can be rewritten as an abstract differential equation in the phase space $\mathscr{C} = C([-\tau,0],X)$ of the form

$$\dot{U} = D\Delta U(t) + L(U_t) + f(U_t), \tag{21}$$

where $D = \text{diag}\{d, d, d\}$, $U_t(\theta) = U(t+\theta)$, $-\tau \le \theta \le 0$, $L : \mathscr{C} \to X$, and $f : \mathscr{C} \to X$ are given, respectively, by

$$L(\varphi) = \begin{pmatrix} -(\mu + \dfrac{\beta_1 I^\star}{1+\alpha I^\star})\varphi_1(0) - \dfrac{\beta_1 S^\star}{(1+\alpha I^\star)^2}\varphi_2(0) \\ \dfrac{\beta_1 I^\star}{1+\alpha I^\star}e^{-\mu\tau}\varphi_1(-\tau) - (\beta_2 R^\star + \mu)\varphi_2(0) + \dfrac{\beta_1 S^\star}{(1+\alpha I^\star)^2}e^{-\mu\tau}\varphi_2(-\tau) - \beta_2 I^\star \varphi_3(0) \\ \beta_2 R^\star \varphi_2(0) + (\beta_2 I^\star - \mu)\varphi_3(0) \end{pmatrix} \tag{22}$$

and

$$f(\varphi) = \begin{pmatrix} \sum_{i+j\ge 2} \dfrac{1}{i!j!} H_{ij}\varphi_1^i(0)\varphi_2^j(0) \\ \sum_{h+i+j+l\ge 2} \dfrac{1}{h!i!j!l!} M_{hijl}\varphi_1^h(-\tau)\varphi_2^i(0)\varphi_2^j(-\tau)\varphi_3^l(0) \\ \sum_{i+j\ge 2} \dfrac{1}{i!j!} N_{ij}\varphi_2^i(0)\varphi_3^j(0) \end{pmatrix}. \tag{23}$$

For $\varphi(\theta) = U_t(\theta)$, $\varphi = (\varphi_1, \varphi_2, \varphi_3)^T \in \mathscr{C}$, the linearized system of (21) at the equilibrium point $(0, 0, 0)$ is

$$\dot{U} = D\Delta U(t) + L(U_t), \tag{24}$$

and its characteristic equation is

$$\lambda y - D\Delta y - L(e^{\lambda \cdot} y) = 0, \tag{25}$$

where $y \in dom(\Delta)$ and $y \neq 0$, $dom(\Delta) \subset X$.

From the properties of the Laplacian operator defined on the bounded domain, the operator Δ on X has the eigenvalues $-\frac{k^2\pi^2}{L^2}$, $k \in N_0 \triangleq \{0, 1, 2\ldots\}$, with the relative eigenfunctions, where

$$\alpha_k^1 = \begin{pmatrix} \varsigma_k \\ 0 \\ 0 \end{pmatrix}, \quad \alpha_k^2 = \begin{pmatrix} 0 \\ \varsigma_k \\ 0 \end{pmatrix},$$
$$\alpha_k^3 = \begin{pmatrix} 0 \\ 0 \\ \varsigma_k \end{pmatrix}, \quad \varsigma_k = \cos\left(\frac{k\pi}{L}x\right). \tag{26}$$

Clearly, $(\alpha_k^1, \alpha_k^2, \alpha_k^3)_0^\infty$ construct a basis of the phase space X. Therefore, any element y in X can be expanded as Fourier series in the following form:

$$y = \sum_{k=0}^{\infty} Y_k^T \begin{pmatrix} \alpha_k^1 \\ \alpha_k^2 \\ \alpha_k^3 \end{pmatrix}, \quad Y_k = \begin{pmatrix} \langle y, \alpha_k^1 \rangle \\ \langle y, \alpha_k^2 \rangle \\ \langle y, \alpha_k^3 \rangle \end{pmatrix}. \tag{27}$$

By calculation

$$L(\varphi^T(\alpha_k^1, \alpha_k^2, \alpha_k^3)^T) = L^T(\varphi)(\alpha_k^1, \alpha_k^2, \alpha_k^3), \quad k \in N_0. \tag{28}$$

According to (26) and (27), (25) is equivalent to

$$\sum_{k=0}^{\infty} Y_k^T \left[\lambda I_3 + D\frac{k^2\pi^2}{L^2} - \begin{pmatrix} -\left(\mu + \dfrac{\beta_1 I^\star}{1+\alpha I^\star}\right) & -\dfrac{\beta_1 S^\star}{(1+\alpha I^\star)^2} & 0 \\ \dfrac{\beta_1 I^\star}{1+\alpha I^\star}e^{-\mu\tau-\lambda\tau} & -\beta_2 R^\star - \mu + \dfrac{\beta_1 S^\star}{(1+\alpha I^\star)^2}e^{-\mu\tau-\lambda\tau} & -\beta_2 I^\star \\ 0 & \beta_2 R^\star & \beta_2 I^\star - \mu \end{pmatrix} \right] \begin{pmatrix} \alpha_k^1 \\ \alpha_k^2 \\ \alpha_k^3 \end{pmatrix} = 0. \tag{29}$$

Therefore, the eigenvalue equation of the linearized system of (20) at $(0, 0, 0)$ is

$$\begin{vmatrix} \lambda + d\dfrac{k^2\pi^2}{L^2} + \mu + \dfrac{\beta_1 I^\star}{1+\alpha I^\star} & \dfrac{\beta_1 S^\star}{(1+\alpha I^\star)^2} & 0 \\ -\dfrac{\beta_1 I^\star}{1+\alpha I^\star}e^{-\mu\tau-\lambda\tau} & \lambda + d\dfrac{k^2\pi^2}{L^2} + \beta_2 R^\star + \mu - \dfrac{\beta_1 S^\star}{(1+\alpha I^\star)^2}e^{-\mu\tau-\lambda\tau} & \beta_2 I^\star \\ 0 & -\beta_2 R^\star & \lambda + d\dfrac{k^2\pi^2}{L^2} - \beta_2 I^\star + \mu \end{vmatrix} = 0. \tag{30}$$

A. Stability analysis of equilibrium point E_0

Here, we shall study the locally asymptotic stability and the globally asymptotic stability of the infection-free equilibrium point E_0. We have the following theorems.

Theorem 3. Let us define $\mathscr{R}_0$ as (17).

(i) If $\mathscr{R}_0 \leq 1$, then the infection-free equilibrium point E_0 is locally asymptotically stable.
(ii) If $\mathscr{R}_0 > 1$, then the infection-free equilibrium point E_0 becomes unstable.

Proof. For the infection-free equilibrium point E_0, the characteristic equation (30) is given by

$$\left(\lambda + d\frac{k^2\pi^2}{L^2} + \mu\right)^2 \left(\lambda + d\frac{k^2\pi^2}{L^2} + \mu - \beta_1 e^{-\lambda\tau}\right) = 0. \tag{31}$$

Clearly, $\lambda_{1,2} = -d\frac{k^2\pi^2}{L^2} - \mu < 0$ are the two roots of this equation. The remaining root is given by the solution of the following transcendental equation:

$$\lambda + d\frac{k^2\pi^2}{L^2} + \mu - \beta_1 e^{-\lambda\tau} = 0. \tag{32}$$

Let $\lambda = r_1 + i\omega_1$ ($\omega_1 > 0$) be a complex root of Eq. (32). Substituting it into Eq. (32) and separating the real and imaginary parts, we have

$$\begin{cases} r_1 + d\frac{k^2\pi^2}{L^2} + \mu = \beta_1 e^{-\mu\tau - r_1\tau}\cos\omega_1\tau, \\ \omega_1 = -\beta_1 e^{-\mu\tau - r_1\tau}\sin\omega_1\tau. \end{cases} \tag{33}$$

Then, we obtain

$$\omega_1^2 + \left(r_1 + d\frac{k^2\pi^2}{L^2} + \mu\right)^2 = \beta_1^2 e^{-2\mu\tau - 2r_1\tau}. \tag{34}$$

Let $\mathscr{R}_0 < 1$. If $r_1 > 0$, then

$$\beta_1^2 e^{-2\mu\tau - 2r_1\tau} = (\beta_1 e^{-\mu\tau})^2 \cdot e^{-2r_1\tau} \leq \mu^2 \cdot e^{-2r_1\tau} < \mu^2.$$

Now, we can see that

$$\omega_1^2 + \left(r_1 + d\frac{k^2\pi^2}{L^2} + \mu\right)^2 < \mu^2,$$

which is impossible. Moreover, if $r_1 = 0$, we have

$$\omega_1^2 = \left(d\frac{k^2\pi^2}{L^2} + \mu + \beta_1 e^{-\mu\tau}\right)\left(-d\frac{k^2\pi^2}{L^2} - \mu + \beta_1 e^{-\mu\tau}\right) < 0.$$

Hence, for $\mathscr{R}_0 < 1$ all the roots of Eq. (32) have negative real parts, and the infection-free equilibrium point E_0 is locally asymptotically stable.

On the other hand, a direct calculation shows that Eq. (32) has a real positive root when $\mathscr{R}_0 > 1$. Indeed, we put

$$\varphi(\lambda) = \lambda + d\frac{k^2\pi^2}{L^2} + \mu - \beta_1 e^{-\mu\tau - \lambda\tau}.$$

Then, $\varphi(0) = \mu - \beta_1 e^{-\mu\tau} < 0$ if $k = 0$, and $\lim_{\lambda\to+\infty}\varphi(\lambda) = +\infty$. Consequently, φ has a positive real root when $k = 0$ and the infection-free equilibrium point E_0 becomes unstable. □

The above theorem only establishes local stability of E_0. However, the following theorem has proved the global asymptotic stability of E_0.

Theorem 4. If $\mathscr{R}_0 \leq 1$, then the infection-free equilibrium point E_0 of system (10) is globally asymptotically stable.

Proof. Let $(S(t,x), I(t,x), R(t,x))$ be any positive solution of system (10) with the homogeneous Neumann boundary conditions (11) and the initial conditions (12).

We consider the following Lyapunov functional:

$$L_1(t) = \int_\Omega \left[S(t,x) - 1 - \ln S(t,x) + e^{\mu\tau}I(t,x) + e^{\mu\tau}R(t,x) + \int_{t-\tau}^{t} \frac{\beta_1 S(\theta,x)I(\theta,x)}{1+\alpha I(\theta,x)}d\theta\right]dx. \tag{35}$$

Calculating the time derivative of $L(t)$ along the positive solution of system (10), we obtain

$$\begin{aligned}
\left.\frac{dL_1(t)}{dt}\right|_{(10)} &= \int_\Omega \left[\left(1 - \frac{1}{S(t,x)}\right)\frac{\partial S(t,x)}{\partial t} + e^{\mu\tau}\frac{\partial I(t,x)}{\partial t} + e^{\mu\tau}\frac{\partial R(t,x)}{\partial t} + \frac{\beta_1 S(t,x)I(t,x)}{1+\alpha I(t,x)} - \frac{\beta_1 S(t-\tau,x)I(t-\tau,x)}{1+\alpha I(t-\tau,x)}\right]dx \\
&= \int_\Omega \Bigg[\mu\,(1 - S(t,x))\left(1 - \frac{1}{S(t,x)}\right) + \left(\frac{\beta_1 I(t,x)}{1+\alpha I(t,x)} - \mu I(t,x)e^{\mu\tau}\right) - \mu e^{\mu\tau}R(t,x) \\
&\quad + d\Delta S(t,x) - d\frac{1}{S(t,x)}\Delta S(t,x) + de^{\mu\tau}\Delta I(t,x) + de^{\mu\tau}\Delta R(t,x)\Bigg]dx \\
&= \int_\Omega \Bigg[\mu\,(1 - S(t,x))\left(1 - \frac{1}{S(t,x)}\right) + \mu e^{\mu\tau}I(t,x)\left(\frac{1}{1+\alpha I(t,x)}R_0 - 1\right) - \mu e^{\mu\tau}R(t,x) \\
&\quad + d\Delta S(t,x) - d\frac{1}{S(t,x)}\Delta S(t,x) + de^{\mu\tau}\Delta I(t,x) + de^{\mu\tau}\Delta R(t,x)\Bigg]dx \\
&\leq \int_\Omega \left[-\frac{\mu\,(S(t,x)-1)^2}{S(t,x)} + \mu e^{\mu\tau}I(t,x)(\mathscr{R}_0 - 1) - \mu e^{\mu\tau}R(t,x)\right]dx \\
&\quad + d\int_\Omega \Delta S(t,x)dx - d\int_\Omega \frac{1}{S(t,x)}\Delta S(t,x)dx + de^{\mu\tau}\int_\Omega \Delta I(t,x)dx + de^{\mu\tau}\int_\Omega \Delta R(t,x)dx.
\end{aligned}$$

Furthermore, according to the divergence theorem and the homogeneous Neumann boundary conditions (11), we have

$$\int_\Omega \Delta S(t,x)dx = \int_{\partial\Omega}\frac{\partial S(t,x)}{\partial n}dx = 0,$$
$$\int_\Omega \Delta I(t,x)dx = \int_{\partial\Omega}\frac{\partial I(t,x)}{\partial n}dx = 0,$$
$$\int_\Omega \Delta R(t,x)dx = \int_{\partial\Omega}\frac{\partial R(t,x)}{\partial n}dx = 0,$$

and

$$\begin{aligned}0 &= \int_{\partial\Omega}\frac{1}{S(t,x)}\nabla S(t,x)\cdot n dx\\ &= \int_\Omega \operatorname{div}\left(\frac{1}{S(t,x)}\nabla S(t,x)\right)dx\\ &= \int_\Omega\left(\frac{1}{S(t,x)}\Delta S(t,x) - \frac{\|\nabla S(t,x)\|^2}{S^2(t,x)}\right)dx.\end{aligned}$$

Thus,

$$\int_\Omega \frac{1}{S(t,x)}\Delta S(t,x)dx = \int_\Omega \frac{\|\nabla S(t,x)\|^2}{S^2(t,x)}dx \ge 0.$$

Now, we can further calculate $\left.\frac{dL_1(t)}{dt}\right|_{(10)}$, that is,

$$\left.\frac{dL_1(t)}{dt}\right|_{(10)} \le \int_\Omega\left[-\frac{\mu\,(S(t,x)-1)^2}{S(t,x)} + \mu e^{\mu\tau}I(t,x)(\mathscr{R}_0 - 1) - \mu e^{\mu\tau}R(t,x)\right]dx - d\int_\Omega\frac{\|\nabla S(t,x)\|^2}{S^2(t,x)}dx.$$

Since $\mathscr{R}_0 \le 1$, we obtain $\left.\frac{dL_1(t)}{dt}\right|_{(10)} \le 0$. Obviously, the equality holds only for $S = 1$, $I = 0$, and $R = 0$. Therefore, by LaSalle's invariance principle, we conclude that the infection-free equilibrium point E_0 is globally asymptotically stable. □

B. Stability analysis of equilibrium point E_1

In the following, we shall discuss the locally asymptotic stability and the globally asymptotic stability of equilibrium point E_1. We have the following theorems.

Theorem 5. (i) If $\mathscr{R}_0 > 1$ and $\mathscr{R}_1 \le 1$, then the equilibrium point E_1 is locally asymptotically stable.
(ii) If $\mathscr{R}_1 > 1$, then equilibrium point E_1 is unstable.

Proof. For equilibrium point E_1, the characteristic equation (30) can be rewritten as

$$\left[\lambda + d\frac{k^2\pi^2}{L^2} + \frac{\mu(\beta_1+\beta_2+\mu\alpha) - \beta_1\beta_2 e^{-\mu\tau}}{\beta_1+\mu\alpha}\right]\left\{\lambda^2 + \left(2d\frac{k^2\pi^2}{L^2} + \mu + \frac{\beta_1+\mu\alpha}{\alpha+e^{\mu\tau}}\right)\lambda + d^2\frac{k^4\pi^4}{L^4} + \left(\mu + \frac{\beta_1+\mu\alpha}{\alpha+e^{\mu\tau}}\right)d\frac{k^2\pi^2}{L^2} + \frac{\mu(\beta_1+\mu\alpha)}{\alpha+e^{\mu\tau}} - \left[\lambda + d\frac{k^2\pi^2}{L^2} + \frac{\beta_1+\mu\alpha-(\beta_1 e^{-\mu\tau}-\mu)e^{\mu\tau}}{\alpha+e^{\mu\tau}}\right]\frac{\mu(\beta_1+\mu\alpha)e^{-\lambda\tau}}{\beta_1(1+\alpha e^{-\mu\tau})}\right\} = 0. \tag{36}$$

Clearly,

$$\lambda = -d\frac{k^2\pi^2}{L^2} - \frac{\mu(\beta_1+\beta_2+\mu\alpha) - \beta_1\beta_2 e^{-\mu\tau}}{\beta_1+\mu\alpha} \tag{37}$$

is a root of Eq. (36), and if $\mathscr{R}_1 \le 1$, then it is a negative real root for any $k = 1, 2, 3 \ldots$.

Now, we discuss the following equation:

$$\lambda^2 + \left(2d\frac{k^2\pi^2}{L^2} + \mu + \frac{\beta_1+\mu\alpha}{\alpha+e^{\mu\tau}}\right)\lambda + d^2\frac{k^4\pi^4}{L^4} + \left(\mu + \frac{\beta_1+\mu\alpha}{\alpha+e^{\mu\tau}}\right)d\frac{k^2\pi^2}{L^2} + \frac{\mu(\beta_1+\mu\alpha)}{\alpha+e^{\mu\tau}} - \left[\lambda + d\frac{k^2\pi^2}{L^2} + \frac{\beta_1+\mu\alpha-(\beta_1 e^{-\mu\tau}-\mu)e^{\mu\tau}}{\alpha+e^{\mu\tau}}\right]\frac{\mu(\beta_1+\mu\alpha)e^{-\lambda\tau}}{\beta_1(1+\alpha e^{-\mu\tau})} = 0. \tag{38}$$

Let $\lambda = r_2 + i\omega_2$ $(\omega_2 > 0)$ be a complex root of Eq. (38). Substituting it into Eq. (38) and separating the real and imaginary parts show that

$$\begin{cases} r_2^2 - \omega_2^2 + r_2\left(2d\frac{k^2\pi^2}{L^2} + \mu + \frac{\beta_1+\mu\alpha}{\alpha+e^{\mu\tau}}\right) + d^2\frac{k^4\pi^4}{L^4} + \left(\mu + \frac{\beta_1+\mu\alpha}{\alpha+e^{\mu\tau}}\right)d\frac{k^2\pi^2}{L^2} + \frac{\mu(\beta_1+\mu\alpha)}{\alpha+e^{\mu\tau}} \\ \quad = \frac{\mu(\beta_1+\mu\alpha)e^{-r_2\tau}}{\beta_1(1+\alpha e^{-\mu\tau})}\left[\left(d\frac{k^2\pi^2}{L^2} + r_2 + \mu\right)\cos\omega_2\tau + \omega_2\sin\omega_2\tau\right], \\ 2r_2\omega_2 + \omega_2\left(2d\frac{k^2\pi^2}{L^2} + \mu + \frac{\beta_1+\mu\alpha}{\alpha+e^{\mu\tau}}\right) = \frac{\mu(\beta_1+\mu\alpha)e^{-r_2\tau}}{\beta_1(1+\alpha e^{-\mu\tau})}\left[\omega_2\cos\omega_2\tau - \left(d\frac{k^2\pi^2}{L^2} + r_2 + \mu\right)\sin\omega_2\tau\right]. \end{cases} \tag{39}$$

Let $\mathscr{R}_0 > 1$, if $r_2 > 0$, then (39) implies

$$\omega_2^4 + 2\omega_2^2\left[r_2^2 + r_2\left(2d\frac{k^2\pi^2}{L^2} + \mu + \frac{\beta_1+\mu\alpha}{\alpha+e^{\mu\tau}}\right) + d^2\frac{k^4\pi^4}{L^4} + \left(\mu + \frac{\beta_1+\mu\alpha}{\alpha+e^{\mu\tau}}\right)d\frac{k^2\pi^2}{L^2} + \frac{\mu(\beta_1+\mu\alpha)}{\alpha+e^{\mu\tau}}\right]$$
$$+\omega_2^2\left[\mu^2 + \left(\frac{\beta_1+\mu\alpha}{\alpha+e^{\mu\tau}}\right)^2\right] + \left[d^2\frac{k^4\pi^4}{L^4} + 2\left(r_2+\mu+\frac{\beta_1+\mu\alpha}{\alpha+e^{\mu\tau}}\right)d\frac{k^2\pi^2}{L^2} + r_2^2 + r_2\left(\mu+\frac{\beta_1+\mu\alpha}{\alpha+e^{\mu\tau}}\right) + \frac{\mu(\beta_1+\mu\alpha)}{\alpha+e^{\mu\tau}}\right]^2$$
$$= \left[\frac{\mu e^{-r_2\tau}(\beta_1+\mu\alpha)}{\beta_1 e^{-\mu\tau}(\alpha+e^{\mu\tau})}\right]^2\cdot\left[\omega_2^2 + \left(d\frac{k^2\pi^2}{L^2} + r_2 + \mu\right)^2\right]$$
$$< \left[\frac{(\beta_1+\mu\alpha)e^{-r_2\tau}}{\alpha+e^{\mu\tau}}\right]^2\cdot\left[\omega_2^2 + \left(d\frac{k^2\pi^2}{L^2} + r_2 + \mu\right)^2\right]$$
$$< \frac{(\beta_1+\mu\alpha)^2}{(\alpha+e^{\mu\tau})^2}\cdot\left[\omega_2^2 + \left(d\frac{k^2\pi^2}{L^2} + r_2 + \mu\right)^2\right].$$

That is to say,

$$\omega_2^4 + 2\omega_2^2\left[d^2\frac{k^4\pi^4}{L^4} + \left(2r_2+\mu+\frac{\beta_1+\mu\alpha}{\alpha+e^{\mu\tau}}\right)d\frac{k^2\pi^2}{L^2} + r_2\left(r_2++\mu+\frac{\beta_1+\mu\alpha}{\alpha+e^{\mu\tau}}\right) + \mu\left(\frac{1}{2}\mu + \frac{\beta_1+\mu\alpha}{\alpha+e^{\mu\tau}}\right)\right]$$
$$\times\left[d^2\frac{k^4\pi^4}{L^4} + \left(2r_2+2\mu+\frac{\beta_1+\mu\alpha}{\alpha+e^{\mu\tau}}\right)d\frac{k^2\pi^2}{L^2} + r_2(r_2+\mu)\right]\cdot\left\{d^2\frac{k^4\pi^4}{L^4} + \left[2r_2+2\mu+\frac{3(\beta_1+\mu\alpha)}{\alpha+e^{\mu\tau}}\right]d\frac{k^2\pi^2}{L^2}\right.$$
$$\left.+r_2\left[r_2+\mu+\frac{2(\beta_1+\mu\alpha)}{\alpha+e^{\mu\tau}}\right] + \frac{2\mu(\beta_1+\mu\alpha)}{\alpha+e^{\mu\tau}}\right\} < 0, \quad (40)$$

which is impossible.

If $r_2 = 0$, we have

$$\omega_2^4 + \omega_2^2\left\{2\left[d^2\frac{k^4\pi^4}{L^4} + \left(\mu+\frac{\beta_1+\mu\alpha}{\alpha+e^{\mu\tau}}\right)d\frac{k^2\pi^2}{L^2}\right] + \mu^2 + \frac{(\beta_1+\alpha\mu)^2}{\beta_1^2(\alpha+e^{\mu\tau})^2}(\beta_1+\mu e^{\mu\tau})(\beta_1-\mu e^{\mu\tau})\right\}$$
$$+\left[d^2\frac{k^4\pi^4}{L^4} + \left(\mu+\frac{\beta_1+\mu\alpha}{\alpha+e^{\mu\tau}}\right)d\frac{k^2\pi^2}{L^2} + \frac{\mu(\beta_1+\alpha\mu)}{\alpha+e^{\mu\tau}} + \frac{\mu(\beta_1+\mu\alpha)(d\frac{k^2\pi^2}{L^2}+\mu)}{\beta_1(1+\alpha e^{-\mu\tau})}\right]$$
$$\cdot\left\{d^2\frac{k^4\pi^4}{L^4} + \left[\mu+\frac{(\beta_1+\mu\alpha)(\beta_1-\mu e^{\mu\tau})}{\beta_1(\alpha+e^{\mu\tau})}\right]d\frac{k^2\pi^2}{L^2} + \frac{\mu(\beta_1+\mu\alpha)(\beta_1-\mu e^{\mu\tau})}{\beta_1(\alpha+e^{\mu\tau})}\right\} = 0. \quad (41)$$

$\mathscr{R}_0 > 1$ implies that Eq. (41) has no positive roots about ω_2, and hence Eq. (38) has no purely imaginary roots.

To sum up, for $\mathscr{R}_0 > 1$ and $\mathscr{R}_1 \le 1$ all the roots of Eq. (36) have negative real parts with $k = 1, 2, 3 \ldots$, and then equilibrium point E_1 is locally asymptotically stable.

On the other hand, obviously if $\mathscr{R}_1 > 1$, then from Eq. (37), we know that Eq. (36) has a positive real solution when $k = 0$. Thus, E_1 is unstable. □

Further, we can obtain the global stability of E_1 as follows.

Theorem 6. If $\mathscr{R}_0 > 1$ and $\mathscr{R}_1 \le 1$, then the equilibrium point E_1 of system (10) is globally asymptotically stable. That is to say, for any initial values $S_0(t,x) \ge 0$, $I_0(t,x) \ge 0$, $R_0(t,x) \ge 0$ and $S_0(t,x) \not\equiv 0$, $I_0(t,x) \not\equiv 0$, $R_0(t,x) \not\equiv 0$, it shows that

$$\lim_{t\to+\infty}(S(t,x), I(t,x), R(t,x)) = \left(\frac{\mu\alpha+\mu e^{\mu\tau}}{\beta_1+\mu\alpha}, \frac{-\mu+\beta_1 e^{-\mu\tau}}{\beta_1+\mu\alpha}, 0\right). \quad (42)$$

Proof. Obviously, if $\mathscr{R}_1 \le 1$ holds, then there is no interior equilibrium point E_2.

Let $(S(t,x), I(t,x), R(t,x))$ be any positive solution of system (10) with the homogeneous Neumann boundary conditions (11) and the initial conditions (12).

Construct a Lyapunov functional

$$L_2(t) = \int_\Omega (L_{21}(t,x) + L_{22}(t,x))dx, \quad (43)$$

where

$$L_{21}(t,x) = S(t,x) - S^* - S^*\ln\frac{S(t,x)}{S^*} + e^{\mu\tau}\left(I(t,x) - I^* - I^*\ln\frac{I(t,x)}{I^*}\right) + e^{\mu\tau}R(t,x)$$

and

$$L_{22}(t,x) = \int_{t-\tau}^{t}\left[\frac{\beta_1 S(\theta,x)I(\theta,x)}{1+\alpha I(\theta,x)} - \frac{\beta_1 S^* I^*}{1+\alpha I^*} - \frac{\beta_1 S^* I^*}{1+\alpha I^*}\ln\frac{(1+\alpha I^*)S(\theta,x)I(\theta,x)}{S^*I^*(1+\alpha I(\theta,x))}\right]d\theta,$$

where

$$S^* = \frac{\mu\alpha + \mu e^{\mu\tau}}{\beta_1 + \mu\alpha}, \quad I^* = \frac{-\mu + \beta_1 e^{-\mu\tau}}{\beta_1 + \mu\alpha}, \quad R^* = 0.$$

In the following calculation, we will use the equilibrium equations

$$\begin{aligned} &\mu - \frac{\beta_1 S^* I^*}{1+\alpha I^*} - \mu S^* = 0, \\ &\mu I^* = \frac{\beta_1 S^* I^*}{1+\alpha I^*} e^{-\mu\tau}, \\ &R^* = 0. \end{aligned}$$

Calculating the derivative of $L_2(t)$ along positive solutions of system (10), we have

$$\begin{aligned}
\left.\frac{dL_2(t)}{dt}\right|_{(10)} &= \int_\Omega \Bigg[\left(1 - \frac{S^*}{S(t,x)}\right)\frac{\partial S(t,x)}{\partial t} + e^{\mu\tau}\left(1 - \frac{I^*}{I(t,x)}\right)\frac{\partial I(t,x)}{\partial t} + e^{\mu\tau}\frac{\partial R(t,x)}{\partial t} \\
&\quad + \frac{\beta_1 S(t,x)I(t,x)}{1+\alpha I(t,x)} - \frac{\beta_1 S(t-\tau,x)I(t-\tau,x)}{1+\alpha I(t-\tau,x)} + \frac{\beta_1 S^* I^*}{1+\alpha I^*}\ln\frac{(1+\alpha I(t,x))S(t-\tau,x)I(t-\tau,x)}{S(t,x)I(t,x)(1+\alpha I(t-\tau,x))}\Bigg] dx \\
&= \int_\Omega \Bigg[\left(1 - \frac{S^*}{S(t,x)}\right)\left(\mu - \frac{\beta_1 S(t,x)I(t,x)}{1+\alpha I(t,x)} - \mu S(t,x)\right) + e^{\mu\tau}\left(\beta_2 I(t,x)R(t,x) - \mu R(t,x)\right) \\
&\quad + e^{\mu\tau}\left(1 - \frac{I^*}{I(t,x)}\right)\left(\frac{\beta_1 e^{-\mu\tau} S(t-\tau,x)I(t-\tau,x)}{1+\alpha I(t-\tau,x)} - \beta_2 I(t,x)R(t,x) - \mu I(t,x)\right) \\
&\quad + d\left(1 - \frac{S^*}{S(t,x)}\right)\Delta S(t,x) + d e^{\mu\tau}\left(1 - \frac{I^*}{I(t,x)}\right)\Delta I(t,x) + d e^{\mu\tau}\Delta R(t,x) \\
&\quad + \frac{\beta_1 S(t,x)I(t,x)}{1+\alpha I(t,x)} - \frac{\beta_1 S(t-\tau,x)I(t-\tau,x)}{1+\alpha I(t-\tau,x)} + \frac{\beta_1 S^* I^*}{1+\alpha I^*}\ln\frac{(1+\alpha I(t,x))S(t-\tau,x)I(t-\tau,x)}{S(t,x)I(t,x)(1+\alpha I(t-\tau,x))}\Bigg] dx \\
&= \int_\Omega \Bigg[\left(1 - \frac{S^*}{S(t,x)}\right)\left(-\mu(S(t,x) - S^*) - \frac{\beta_1 S(t,x)I(t,x)}{1+\alpha I(t,x)} + \frac{\beta_1 S^* I^*}{1+\alpha I^*}\right) + e^{\mu\tau}\left(\beta_2 I(t,x)R(t,x) - \mu R(t,x)\right) \\
&\quad + e^{\mu\tau}\left(1 - \frac{I^*}{I(t,x)}\right)\left(\frac{\beta_1 e^{-\mu\tau} S(t-\tau,x)I(t-\tau,x)}{1+\alpha I(t-\tau,x)} - \beta_2 I(t,x)R(t,x) - \mu I(t,x)\right) \\
&\quad + d\left(1 - \frac{S^*}{S(t,x)}\right)\Delta S(t,x) + d e^{\mu\tau}\left(1 - \frac{I^*}{I(t,x)}\right)\Delta I(t,x) + d e^{\mu\tau}\Delta R(t,x) \\
&\quad + \frac{\beta_1 S(t,x)I(t,x)}{1+\alpha I(t,x)} - \frac{\beta_1 S(t-\tau,x)I(t-\tau,x)}{1+\alpha I(t-\tau,x)} + \frac{\beta_1 S^* I^*}{1+\alpha I^*}\ln\frac{(1+\alpha I(t,x))S(t-\tau,x)I(t-\tau,x)}{S(t,x)I(t,x)(1+\alpha I(t-\tau,x))}\Bigg] dx \\
&= \int_\Omega \Bigg[\left(1 - \frac{S^*}{S(t,x)}\right)(-\mu(S(t,x) - S^*)) + \frac{\beta_1 S^* I^*}{1+\alpha I^*}\left(1 - \frac{S^*}{S(t,x)}\right) + \frac{\beta_1 S^* I(t,x)}{1+\alpha I(t,x)} - \frac{\beta_1 I^* S(t-\tau,x)I(t-\tau,x)}{I(t-\tau,x)(1+\alpha I(t-\tau,x))} \\
&\quad - \mu e^{\mu\tau} I(t,x) + \beta_2 e^{\mu\tau} I^* R(t,x) + \mu e^{\mu\tau} I^* - \mu e^{\mu\tau} R(t,x) + \frac{\beta_1 S^* I^*}{1+\alpha I^*}\ln\frac{(1+\alpha I(t,x))S(t-\tau,x)I(t-\tau,x)}{S(t,x)I(t,x)(1+\alpha I(t-\tau,x))} \\
&\quad + d\left(1 - \frac{S^*}{S(t,x)}\right)\Delta S(t,x) + d e^{\mu\tau}\left(1 - \frac{I^*}{I(t,x)}\right)\Delta I(t,x) + d e^{\mu\tau}\Delta R(t,x)\Bigg] dx \\
&= \int_\Omega \Bigg[-\mu\frac{(S(t,x) - S^*)^2}{S(t,x)} + \frac{\beta_1 S^* I(t,x)}{1+\alpha I(t,x)} - \frac{\beta_1 S^* I^*}{1+\alpha I^*}\left(\frac{S^*}{S(t,x)} - 1\right) - \frac{\beta_1 I^* S(t-\tau,x)I(t-\tau,x)}{I(t,x)(1+\alpha I(t-\tau,x))} - \mu e^{\mu\tau} I(t,x) \\
&\quad + \mu e^{\mu\tau} I^* + \frac{\mu e^{\mu\tau}(\beta_1 + \beta_2 + \mu\alpha)(\mathscr{R}_1 - 1)R(t,x)}{\beta_1 + \mu\alpha} + \frac{\beta_1 S^* I^*}{1+\alpha I^*}\ln\frac{(1+\alpha I(t,x))S(t-\tau,x)I(t-\tau,x)}{S(t,x)I(t,x)(1+\alpha I(t-\tau,x))} \\
&\quad + d\left(1 - \frac{S^*}{S(t,x)}\right)\Delta S(t,x) + d e^{\mu\tau}\left(1 - \frac{I^*}{I(t,x)}\right)\Delta I(t,x) + d e^{\mu\tau}\Delta R(t,x)\Bigg] dx
\end{aligned}$$

$$
\begin{aligned}
&= \int_\Omega \Bigg[-\mu \frac{(S(t,x)-S^*)^2}{S(t,x)} + \frac{\beta_1 S^* I(t,x)}{1+\alpha I(t,x)} - \frac{\beta_1 S^* I^*}{1+\alpha I^*}\left(\frac{S^*}{S(t,x)} - 1 - \ln\frac{S^*}{S(t,x)}\right) - \frac{\beta_1 I^* S(t-\tau,x) I(t-\tau,x)}{I(t,x)(1+\alpha I(t-\tau,x))} \\
&\quad - \mu e^{\mu\tau} I(t,x) + \mu e^{\mu\tau} I^* + \frac{\mu e^{\mu\tau}(\beta_1+\beta_2+\mu\alpha)(\mathscr{R}_1-1)R(t,x)}{\beta_1+\mu\alpha} + \frac{\beta_1 S^* I^*}{1+\alpha I^*}\ln\frac{(1+\alpha I(t,x))S(t-\tau,x)I(t-\tau,x)}{S^* I(t,x)(1+\alpha I(t-\tau,x))} \\
&\quad + d\left(1-\frac{S^*}{S(t,x)}\right)\Delta S(t,x) + de^{\mu\tau}\left(1-\frac{I^*}{I(t,x)}\right)\Delta I(t,x) + de^{\mu\tau}\Delta R(t,x)\Bigg] dx \\
&= \int_\Omega \Bigg[-\mu \frac{(S(t,x)-S^*)^2}{S(t,x)} + \frac{\beta_1 S^* I(t,x)}{1+\alpha I(t,x)} - \frac{\beta_1 S^* I^*}{1+\alpha I^*}\left(\frac{S^*}{S(t,x)} - 1 - \ln\frac{S^*}{S(t,x)}\right) + \mu e^{\mu\tau} I^* - \mu e^{\mu\tau} I(t,x) \\
&\quad - \frac{\beta_1 S^* I^*}{1+\alpha I^*}\left(\frac{I^*(1+\alpha I^*)S(t-\tau,x)I(t-\tau,x)}{S^* I^* I(t,x)(1+\alpha I(t-\tau,x))} - 1 - \ln\frac{I^*(1+\alpha I^*)S(t-\tau,x)I(t-\tau,x)}{S^* I^* I(t,x)(1+\alpha I(t-\tau,x))}\right) - \frac{\beta_1 S^* I^*}{1+\alpha I^*} \\
&\quad + \frac{\mu e^{\mu\tau}(\beta_1+\beta_2+\mu\alpha)(\mathscr{R}_1-1)R(t,x)}{\beta_1+\mu\alpha} + \frac{\beta_1 S^* I^*}{1+\alpha I^*}\ln\frac{1+\alpha I(t,x)}{1+\alpha I^*} \\
&\quad + d\left(1-\frac{S^*}{S(t,x)}\right)\Delta S(t,x) + de^{\mu\tau}\left(1-\frac{I^*}{I(t,x)}\right)\Delta I(t,x) + de^{\mu\tau}\Delta R(t,x)\Bigg] dx \\
&= \int_\Omega \Bigg[-\mu \frac{(S(t,x)-S^*)^2}{S(t,x)} - \frac{\beta_1 S^* I^*}{1+\alpha I^*}\left(\frac{S^*}{S(t,x)} - 1 - \ln\frac{S^*}{S(t,x)}\right) - \frac{\beta_1 S^* I^*}{1+\alpha I^*}\left(\frac{1+\alpha I(t,x)}{1+\alpha I^*} - 1 - \ln\frac{1+\alpha I(t,x)}{1+\alpha I^*}\right) \\
&\quad - \frac{\beta_1 S^* I^*}{1+\alpha I^*}\left(\frac{I^*(1+\alpha I^*)S(t-\tau,x)I(t-\tau,x)}{S^* I^* I(t,x)(1+\alpha I(t-\tau,x))} - 1 - \ln\frac{I^*(1+\alpha I^*)S(t-\tau,x)I(t-\tau,x)}{S^* I^* I(t,x)(1+\alpha I(t-\tau,x))}\right) + \frac{\beta_1 S^* I(t,x)}{1+\alpha I(t,x)} \\
&\quad - \mu e^{\mu\tau} I(t,x) + \frac{\beta_1 S^* I^*(1+\alpha I(t,x))}{(1+\alpha I^*)^2} - \frac{\beta_1 S^* I^*}{1+\alpha I^*} + \frac{\mu e^{\mu\tau}(\beta_1+\beta_2+\mu\alpha)(\mathscr{R}_1-1)R(t,x)}{\beta_1+\mu\alpha} \\
&\quad + d\left(1-\frac{S^*}{S(t,x)}\right)\Delta S(t,x) + de^{\mu\tau}\left(1-\frac{I^*}{I(t,x)}\right)\Delta I(t,x) + de^{\mu\tau}\Delta R(t,x)\Bigg] dx \\
&= \int_\Omega \Bigg[-\mu \frac{(S(t,x)-S^*)^2}{S(t,x)} - \frac{\beta_1 S^* I^*}{1+\alpha I^*}\left(\frac{S^*}{S(t,x)} - 1 - \ln\frac{S^*}{S(t,x)}\right) - \frac{\beta_1 S^* I^*}{1+\alpha I^*}\left(\frac{1+\alpha I(t,x)}{1+\alpha I^*} - 1 - \ln\frac{1+\alpha I(t,x)}{1+\alpha I^*}\right) \\
&\quad - \frac{\beta_1 S^* I^*}{1+\alpha I^*}\left(\frac{I^*(1+\alpha I^*)S(t-\tau,x)I(t-\tau,x)}{S^* I^* I(t,x)(1+\alpha I(t-\tau,x))} - 1 - \ln\frac{I^*(1+\alpha I^*)S(t-\tau,x)I(t-\tau,x)}{S^* I^* I(t,x)(1+\alpha I(t-\tau,x))}\right) \\
&\quad + \beta_1 S^* I(t,x)\left(\frac{1}{1+\alpha I(t,x)} - \frac{1}{1+\alpha I^*}\right) + \frac{\beta_1 S^* I^*}{1+\alpha I^*}\left(\frac{1+\alpha I(t,x)}{1+\alpha I^*} - 1\right) + \frac{\mu e^{\mu\tau}(\beta_1+\beta_2+\mu\alpha)(\mathscr{R}_1-1)R(t,x)}{\beta_1+\mu\alpha} \\
&\quad + d\left(1-\frac{S^*}{S(t,x)}\right)\Delta S(t,x) + de^{\mu\tau}\left(1-\frac{I^*}{I(t,x)}\right)\Delta I(t,x) + de^{\mu\tau}\Delta R(t,x)\Bigg] dx \\
&= \int_\Omega \Bigg[-\mu \frac{(S(t,x)-S^*)^2}{S(t,x)} - \frac{\beta_1 S^* I^*}{1+\alpha I^*}\left(\frac{S^*}{S(t,x)} - 1 - \ln\frac{S^*}{S(t,x)}\right) - \frac{\beta_1 S^* I^*}{1+\alpha I^*}\left(\frac{1+\alpha I(t,x)}{1+\alpha I^*} - 1 - \ln\frac{1+\alpha I(t,x)}{1+\alpha I^*}\right) \\
&\quad - \frac{\beta_1 S^* I^*}{1+\alpha I^*}\left(\frac{I^*(1+\alpha I^*)S(t-\tau,x)I(t-\tau,x)}{S^* I^* I(t,x)(1+\alpha I(t-\tau,x))} - 1 - \ln\frac{I^*(1+\alpha I^*)S(t-\tau,x)I(t-\tau,x)}{S^* I^* I(t,x)(1+\alpha I(t-\tau,x))}\right) \\
&\quad - \frac{\alpha\beta_1 S^*(I(t,x)-I^*)^2}{(1+\alpha I^*)^2(1+\alpha I(t,x))} + \frac{\mu e^{\mu\tau}(\beta_1+\beta_2+\mu\alpha)(\mathscr{R}_1-1)R(t,x)}{\beta_1+\mu\alpha} \\
&\quad + d\left(1-\frac{S^*}{S(t,x)}\right)\Delta S(t,x) + de^{\mu\tau}\left(1-\frac{I^*}{I(t,x)}\right)\Delta I(t,x) + de^{\mu\tau}\Delta R(t,x)\Bigg] dx.
\end{aligned}
$$

Now, we consider a function

$$g(\xi) = \xi - 1 - \ln \xi. \tag{44}$$

Note that $g(\xi)$ has a global minimum at $\xi = 1$ and satisfies $g(1) = 0$. Moreover, the function $g(\xi)$ tends to infinity as its argument tends to 0 or infinity. Thus, we have

$$g\left(\frac{S^*}{S(t,x)}\right) \geq 0, \quad g\left(\frac{1+\alpha I(t,x)}{1+\alpha I^*}\right) \geq 0$$

and

$$g\left(\frac{I^*(1+\alpha I^*)S(t-\tau,x)I(t-\tau,x)}{S^*I^*I(t,x)(1+\alpha I(t-\tau,x))}\right) \geq 0.$$

Similar to the proof of Theorem 4, by the divergence theorem and the homogeneous Neumann boundary conditions (11), we have

$$\int_\Omega \left[d\left(1-\frac{S^*}{S(t,x)}\right)\Delta S(t,x) + de^{\mu\tau}\left(1-\frac{I^*}{I(t,x)}\right)\Delta I(t,x) + de^{\mu\tau}\Delta R(t,x)\right]dx \leq 0.$$

Therefore, under the conditions $\mathscr{R}_0 > 1$ and $\mathscr{R}_1 \leq 1$, we obtain

$$\left.\frac{dL_2(t)}{dt}\right|_{(10)} \leq 0.$$

We now use LaSalle's invariance principle and determine the largest invariant subset $\mathscr{D}_0$ of $\mathscr{D} = \{(S(t,x), I(t,x), R(t,x)) : \frac{dL_2(t)}{dt} = 0\}$. Obviously, if and only if $S(t,x) = S^*$, $I(t,x) = I^*$ and $R(t,x) = R^*$, we have $\frac{dL_2(t)}{dt} = 0$. Therefore, equilibrium point E_1 of system (10) is globally asymptotically stable. That is to say, Eq. (42) holds. □

C. Stability analysis of equilibrium point E_2

The interior equilibrium point E_2 is important, since in an online social network susceptible users, infected users, and recovered users can always coexist. In the following, we focus on the local stability of the interior equilibrium point E_2.

Define

$$a_1 = \frac{\mu(\beta_1+\beta_2+\mu\alpha)}{\beta_2+\mu\alpha} + \frac{\beta_1\beta_2 e^{-\mu\tau}}{\beta_1+\beta_2+\mu\alpha},$$

$$a_2 = \frac{\mu\beta_1\beta_2 e^{-\mu\tau}(\beta_1+2\beta_2+2\mu\alpha)}{(\beta_2+\alpha)(\beta_1+\beta_2+\mu\alpha)} - \mu^2,$$

$$a_3 = \frac{\mu^2[\beta_1\beta_2 e^{-\mu\tau} - \mu(\beta_1+\beta_2+\mu\alpha)]}{\beta_2+\mu\alpha},$$

$$a_4 = \frac{\beta_1\beta_2^2 e^{-\mu\tau}}{(\beta_2+\mu\alpha)(\beta_1+\beta_2+\mu\alpha)}.$$

Clearly, $a_1 > 0$, $a_2 > 0$, $a_3 > 0$, and $a_4 > 0$, since $\mathscr{R}_1 > 1$.

A simple calculation shows that the characteristic equation (30) at the interior equilibrium point E_2 has the following form:

$$\lambda^3 + \left(3d\frac{k^2\pi^2}{L^2} + a_1\right)\lambda^2 + \left(3d^2\frac{k^4\pi^4}{L^4} + 2a_1 d\frac{k^2\pi^2}{L^2} + a_2\right)\lambda + d^3\frac{k^6\pi^6}{L^6} + a_1 d^2\frac{k^4\pi^4}{L^4} + a_2 d\frac{k^2\pi^2}{L^2} + a_3$$
$$- \left[a_4\lambda^2 + \left(2a_4 d\frac{k^2\pi^2}{L^2} + \mu a_4\right)\lambda + a_4 d^2\frac{k^4\pi^4}{L^4} + \mu a_4 d\frac{k^2\pi^2}{L^2}\right]e^{-\lambda\tau} = 0. \tag{45}$$

Let $\lambda = r_3 + i\omega_3$ ($\omega_3 > 0$) be a complex root of Eq. (45). Substituting it into Eq. (45) and separating the real and imaginary parts, we have

$$\begin{cases} -\omega_3^2\left(3d\frac{k^2\pi^2}{L^2} + a_1 + 3r_3\right) + d^3\frac{k^6\pi^6}{L^6} + (3r_3+a_1)d^2\frac{k^4\pi^4}{L^4} + (3r_3^2 + 2r_3a_1 + a_2)d\frac{k^2\pi^2}{L^2} + r_3^3 + r_3^2a_1 + r_3a_2 + a_3 \\ \quad = \left[-\omega_3^2 + d^2\frac{k^4\pi^4}{L^4} + (\mu+2r_3)d\frac{k^2\pi^2}{L^2} + r_3^2 + r_3\mu\right]a_4e^{-r_3\tau}\cos\omega_3\tau + \left(2d\frac{k^2\pi^2}{L^2} + 2r_3 + \mu\right)\omega_3a_4e^{-r_3\tau}\sin\omega_3\tau, \\ -\omega_3^3 + \omega_3\left[3d^2\frac{k^4\pi^4}{L^4} + 2(3r_3+a_1)d\frac{k^2\pi^2}{L^2} + 3r_3^2 + 2r_3a_1 + a_2\right] \\ \quad = \left(2d\frac{k^2\pi^2}{L^2} + 2r_3 + \mu\right)\omega_3a_4e^{-r_3\tau}\cos\omega_3\tau - \left[-\omega_3^2 + d^2\frac{k^4\pi^4}{L^4} + (\mu+2r_3)d\frac{k^2\pi^2}{L^2} + r_3^2 + r_3\mu\right]a_4e^{-r_3\tau}\sin\omega_3\tau. \end{cases} \tag{46}$$

Let $\mathscr{R}_1 > 1$, if $r_3 > 0$, then taking square on both sides of the equations of (46) and summing them up, we obtain

$$\omega_3^6 + \omega_3^4\left[3d^2\frac{k^4\pi^4}{L^4} + 2(3r_3+a_1)d\frac{k^2\pi^2}{L^2} + 3r_3^2 + 2r_3a_1 + a_1^2 - 2a_2 - a_4^2\right] + \omega_3^2\left\{3d^4\frac{k^8\pi^8}{L^8} + 4(a_1+3r_3)d^3\frac{k^6\pi^6}{L^6}\right.$$
$$+ 2(a_1+3r_3+a_4)(a_1+3r_3-a_4)d^2\frac{k^4\pi^4}{L^4} + [4r_3(a_1^2-a_4^2) + 12r_3^2(r_3+a_1) + 2(a_1a_2 - 3a_3 - \mu a_4^2)]d\frac{k^2\pi^2}{L^2}$$
$$\left.+ \left[2r_3^2(a_1^2-a_4^2) + r_3^3(3r_3+4a_1) + 2r_3(a_1a_2 - 3a_3 - \mu a_4^2) + a_2^2 - \mu^2a_4^2 - 2a_1a_3\right]\right\} + \left\{d^3\frac{k^6\pi^6}{L^6} + (3r_3 + a_1\right.$$
$$\left.- a_4)\,d^2\frac{k^4\pi^4}{L^4} + [3r_3^2 + 2r_3(a_1-a_4) + a_2 - \mu a_4]d\frac{k^2\pi^2}{L^2} + [r_3^3 + r_3^2(a_1-a_4) + r_3(a_2-\mu a_4) + a_3]\right\}$$
$$\times\left\{d^3\frac{k^6\pi^6}{L^6} + (3r_3+a_1+a_4)d^2\frac{k^4\pi^4}{L^4} + [3r_3^2 + 2r_3(a_1+a_4) + a_2 - \mu a_4]d\frac{k^2\pi^2}{L^2} + [r_3^3 + r_3^2(a_1+a_4) + r_3(a_2+\mu a_4) + a_3]\right\} < 0. \tag{47}$$

For the further discussion of (47), we give the following necessary lemma.

Lemma 1. Define $\mathscr{R}_1$ as (18).

(i) If $\beta_2 + \mu\alpha - \beta_1 \le 0$, then when $1 < \mathscr{R}_1 \le 1 + \frac{\mu\alpha}{\beta_2}$, we have $a_1^2 - 2a_2 - a_4^2 > 0$, $a_1a_2 - 3a_3 - \mu a_4^2 > 0$, and $a_2^2 - \mu^2 a_4^2 - 2a_1a_3 > 0$.

(ii) If $(\sqrt{2}-1)(\beta_2+\mu\alpha) - \beta_1 < 0$ and $\beta_2 + \mu\alpha - \beta_1 > 0$, then when $1 < \mathscr{R}_1 \le \min\left\{1+\frac{\mu\alpha}{\beta_2}, 2\left(1+\frac{\beta_1}{\beta_2+\mu\alpha-\beta_1}\right)\right\}$, we have $a_1^2 - 2a_2 - a_4^2 > 0$, $a_1a_2 - 3a_3 - \mu a_4^2 > 0$, and $a_2^2 - \mu^2 a_4^2 - 2a_1a_3 > 0$.

Proof. If $1 < \mathscr{R}_1 < 1 + \frac{\mu\alpha}{\beta_2}$, we can calculate that

$$a_1^2 - 2a_2 - a_4^2 = \mu^2\left[(\mathscr{R}_1-1)^2 + \left(1+\frac{\beta_1}{\beta_2+\mu\alpha}\right)^2 + \frac{\beta_2(1-\mathscr{R}_1)+\mu\alpha}{\beta_2+\mu\alpha}\left(1+\frac{\beta_1}{\beta_2+\mu\alpha}\right)\right] > 0.$$

Moreover,

$$a_1a_2 - 3a_3 - \mu a_4^2 = \mu^3\left\{\mathscr{R}_1\left(\mathscr{R}_1 - 1 + \frac{\beta_1\mathscr{R}_1}{\beta_2+\mu\alpha}\right) + \mathscr{R}_1^2\left[1-\frac{\beta_2^2}{(\beta_2+\mu\alpha)^2}\right] + \left(1+\frac{\beta_1}{\beta_2+\mu\alpha}\right)\left(2-\frac{\beta_2+\mu\alpha-\beta_1}{\beta_2+\mu\alpha}\mathscr{R}_1\right)\right\},$$

which implies

(i) if $\beta_2+\mu\alpha-\beta_1 \le 0$, we have $a_1a_2 - 3a_3 - \mu a_4^2 > 0$, or

(ii) if $\beta_2+\mu\alpha-\beta_1 > 0$, we have $a_1a_2 - 3a_3 - \mu a_4^2 > 0$ when $\mathscr{R}_1 \le 2\left(1+\frac{\beta_1}{\beta_2+\mu\alpha-\beta_1}\right)$.

Further, we have

$$a_2^2 - \mu^2a_4^2 - 2a_1a_3 = \mu^4\left\{(\mathscr{R}_1-1)^2 + \mathscr{R}_1^2\left[1-\frac{\beta_2^2}{(\beta_2+\mu\alpha)^2}\right] + \frac{\beta_1\mathscr{R}_1^2}{\beta_2+\mu\alpha}\left(2+\frac{\beta_1}{\beta_2+\mu\alpha}\right) - 2(\mathscr{R}_1-1)\left(1+\frac{\beta_1}{\beta_2+\mu\alpha}\right)^2\right\}.$$

Define

$$f(\mathscr{R}_1) = (A^2-1)\mathscr{R}_1^2 - 2A^2\mathscr{R}_1 + 2A^2, \tag{48}$$

where $A = 1 + \frac{\beta_1}{\beta_2+\mu\alpha} > 1$.

Obviously, $\frac{A^2}{A^2-1} > 1$ and $f\left(\frac{A^2}{A^2-1}\right) = A^2\left(2-\frac{A^2}{A^2-1}\right)$. If $2 - \frac{A^2}{A^2-1} > 0$, that is to say, $(\sqrt{2}-1)(\beta_2+\mu\alpha)-\beta_1 < 0$, then we have $f\left(\frac{A^2}{A^2-1}\right) > 0$ under the condition $\mathscr{R}_1 > 1$. Thus, $a_2^2 - \mu^2a_4^2 - 2a_1a_3 > 0$. This completes the proof. □

On the other hand, we have

$$a_1 - a_4 = \frac{\mu(\beta_1+\beta_2+\mu\alpha)}{\beta_2+\mu\alpha} + \frac{\beta_1\beta_2e^{-\mu\tau}}{\beta_1+\beta_2+\mu\alpha}\left(1-\frac{\beta_2}{\beta_2+\mu\alpha}\right) > 0 \tag{49}$$

and

$$a_2 - \mu a_4 = \frac{\mu(\beta_2+\mu\alpha)[\beta_1\beta_2e^{\mu\tau} - \mu(\beta_1+\beta_2+\mu\alpha)] + \mu\beta_1\beta_2e^{\mu\tau}(\beta_1+\mu\alpha)}{(\beta_2+\mu\alpha)(\beta_1+\beta_2+\mu\alpha)} > 0, \tag{50}$$

if $\mathscr{R}_1 > 1$.

Thus, if the conditions of Lemma 1 hold, then (47) cannot hold. That is to say, all the roots of Eq. (45) have non-positive real parts.

In the following, we will prove that any pure imaginary is not a root of Eq. (45). For $r_3 = 0$, we obtain

$$\begin{aligned}&\omega_3^6 + \omega_3^4\left(3d^2\frac{k^4\pi^4}{L^4} + 2a_1d\frac{k^2\pi^2}{L^2} + a_1^2 - 2a_2 - a_4^2\right) + \omega_3^2\left[3d^4\frac{k^8\pi^8}{L^8} + 4a_1d^3\frac{k^6\pi^6}{L^6} + 2(a_1+a_4)(a_1-a_4)d^2\frac{k^4\pi^4}{L^4}\right.\\ &\left.\times\, 2(a_1a_2 - 3a_3 - \mu a_4^2)d\frac{k^2\pi^2}{L^2} + a_2^2 - \mu^2a_4^2 - 2a_1a_3\right] + \left\{d^3\frac{k^6\pi^6}{L^6} + (a_1-a_4)d^2\frac{k^4\pi^4}{L^4} + (a_2-\mu a_4)d\frac{k^2\pi^2}{L^2} + a_3\right\}\\ &\times\left\{d^3\frac{k^6\pi^6}{L^6} + (a_1+a_4)d^2\frac{k^4\pi^4}{L^4} + (a_2+\mu a_4)d\frac{k^2\pi^2}{L^2} + a_3\right\} = 0.\end{aligned} \tag{51}$$

We can find if the conditions of Lemma 1 hold, then Eq. (51) has no positive solutions. Therefore, all the roots of Eq. (45) have negative real parts based on Lemma 1 and (49) and (50).

Now, we can give the theorem about the local stability of the interior equilibrium point E_2 of system (10) as follows.

Theorem 7. Suppose that the conditions of Lemma 1 hold, then the interior equilibrium point E_2 is locally asymptotically stable.

Remark 2. In order to obtain the local stability of the interior equilibrium point E_2, we constrainedly add some assumptions in Lemma 1. However, we find these assumptions are not sufficient and necessary conditions. That is to say, even if these conditions are not satisfied, E_2 may also be stable.

Next, we will further simplify the stability conditions of the interior equilibrium point E_2 by proving its global stability.

Theorem 8. If $\mathscr{R}_1 > 1$, then the interior equilibrium point E_2 of system (10) is globally asymptotically stable for the initial conditions (12).

Proof. Define a Lyapunov function as follows:

$$L_3(t) = \int_\Omega \left\{ S(t,x) - S^{**} - S^{**} \ln \frac{S(t,x)}{S^{**}} + e^{\mu\tau} \left(I(t,x) - I^{**} - I^{**} \ln \frac{I(t,x)}{I^{**}} \right) + e^{\mu\tau} \left(R(t,x) - R^{**} - R^{**} \ln \frac{R(t,x)}{R^{**}} \right) \right.$$
$$\left. + \int_{t-\tau}^{t} \left[\frac{\beta_1 S(\theta,x) I(\theta,x)}{1+\alpha I(\theta,x)} - \frac{\beta_1 S^{**} I^{**}}{1+\alpha I^{**}} - \frac{\beta_1 S^{**} I^{**}}{1+\alpha I^{**}} \ln \frac{(1+\alpha I^{**}) S(\theta,x) I(\theta,x)}{S^{**} I^{**} (1+\alpha I(\theta,x))} \right] d\theta \right\}, \tag{52}$$

where

$$S^{**} = \frac{\beta_2 + \mu\alpha}{\beta_1 + \beta_2 + \mu\alpha}, \quad I^{**} = \frac{\mu}{\beta_2}, \quad R^{**} = \frac{\beta_1\beta_2 e^{-\mu\tau} - \mu(\beta_1 + \beta_2 + \mu\alpha)}{\beta_2(\beta_1 + \beta_2 + \mu\alpha)}.$$

By $\mathscr{R}_1 > 1$ and the homogeneous Neumann boundary conditions (11), its derivative along the positive solutions of system (10) can be computed as follows:

$$\left.\frac{dL_3(t)}{dt}\right|_{(10)} = \int_\Omega \left\{ -\mu \frac{(S(t,x) - S^{**})^2}{S(t,x)} - \frac{\alpha\beta_1 S^{**} (I(t,x) - I^{**})^2}{(1+\alpha I(t,x))(1+\alpha I^{**})^2} - \frac{\beta_1 S^{**} I^{**}}{1+\alpha I^{**}} \left[g\left(\frac{S^{**}}{S(t,x)} \right) \right.\right.$$
$$\left.\left. + g\left(\frac{1+\alpha I(t,x)}{1+\alpha I^{**}} \right) + g\left(\frac{(1+\alpha I^{**}) S(t-\tau,x) I(t-\tau,x)}{S^{**} I(t,x)(1+\alpha I(t-\tau,x))} \right) \right] \right\} dx - dS^{**} \int_\Omega \frac{\|\nabla S(t,x)\|^2}{S^2(t,x)} dx$$
$$- de^{-\mu\tau} I^{**} \int_\Omega \frac{\|\nabla I(t,x)\|^2}{I^2(t,x)} dx - de^{-\mu\tau} R^{**} \int_\Omega \frac{\|\nabla R(t,x)\|^2}{R^2(t,x)} dx \le 0.$$

It is easy to verify that the largest invariant set in the set $\left.\frac{dL_3(t)}{dt}\right|_{(10)} = 0$ is the interior equilibrium point E_2. Thus, according to LaSalle's invariance principle, we obtain that the interior equilibrium point E_2 of system (10) is globally asymptotically stable. □

V. NUMERICAL SIMULATION

In this section, we simulate and analyze the spatial-temporal dynamic characteristics of system (10) by simulations on Matlab, including the trend in the quantity and spatial distribution of users. Meanwhile, from the view of numerical simulations, we verify the correctness of the theoretical analysis by choosing the different values of parameters in the different simulations.

A. Stability of the infection-free equilibrium point E_0

Consider $L = 5, d = 2, \beta_1 = 0.2, \beta_2 = 0.1, \mu = 0.3, \alpha = 0.5$, and $\tau = 0.2$ in system (10). Obviously, $\mathscr{R}_0 = 0.6278 < 1$. Thus, there only exists an infection-free equilibrium point $E_0 = (1, 0, 0)$, and E_0 is globally asymptotically stable from Theorem 4. As Fig. 3 shows that regardless of the initial densities of susceptible users, infected users, and recovered users in online social networks, there are no infected users and recovered users except susceptible users in the end. That is to say, in this situation rumor cannot continue to spread.

Moreover, it is easy to find that E_0 is stable for any $\tau \ge 0$ as shown in Fig. 4. Meanwhile, $S(t,x)$ and $I(t,x)$ spend less time to converge to constants with τ increasing, and $R(t,x)$ has no any change for different τ. This kind of phenomenon is reasonable. We have supposed that there is a latent period between infected users transmits a rumor to susceptible users and the production of new infected users in the model. Thus, delay should have an important influence on susceptible users and infected users. Moreover, a larger latent period is beneficial to terminate rumor diffusion, which is consistent with the numerical result.

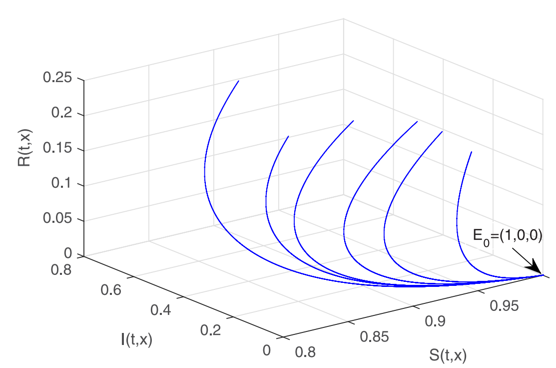

FIG. 3. The infection-free equilibrium point E_0 is globally asymptotically stable.

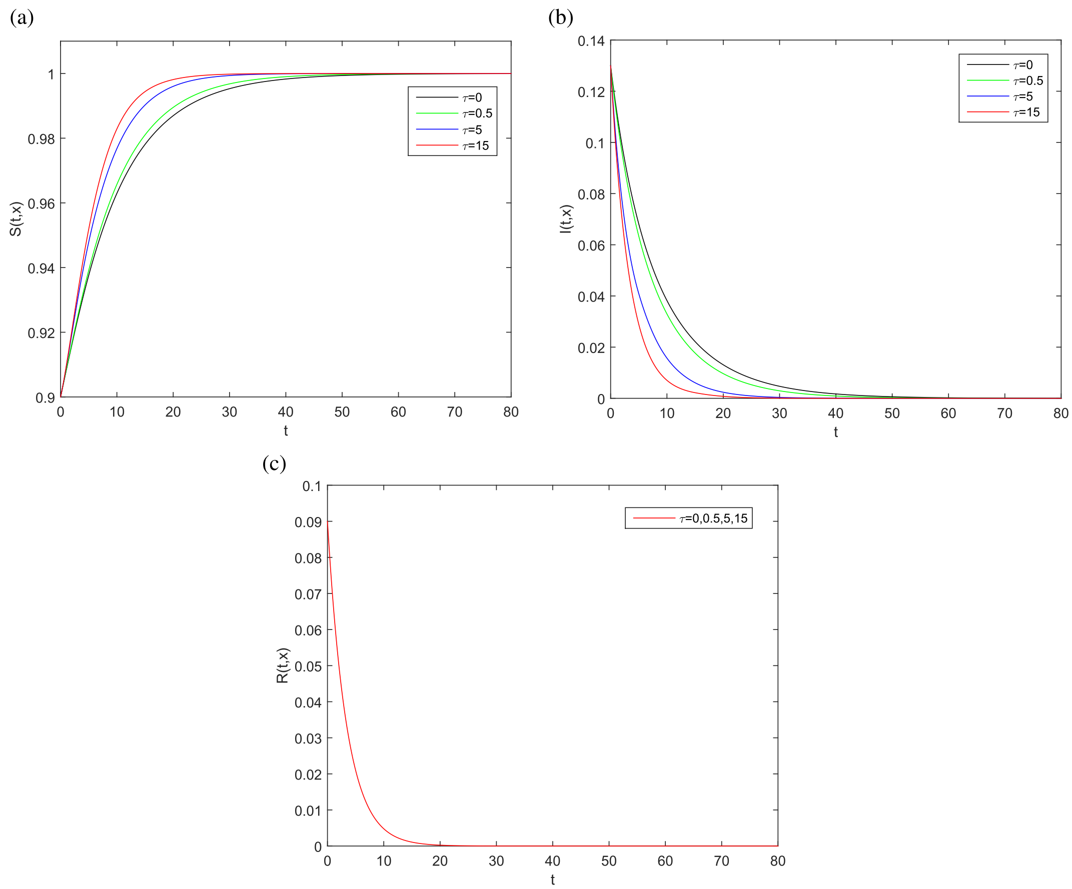

FIG. 4. $S(t,x)$, $I(t,x)$, and $R(t,x)$ converge to constants for different τ.

B. Stability of equilibrium point E_1

Consider $L = 5, d = 1, \beta_1 = 0.4, \beta_2 = 0.2, \mu = 0.35, \alpha = 0.15$ in system (10). A simple calculation shows that if $\tau < 0.3815$, then $\mathscr{R}_0 > 1$, and for any $\tau > 0$ we have $\mathscr{R}_1 \le 1$. Thus, equilibrium point E_1 is globally asymptotically stable for $\tau < 0.3815$. We take $\tau = 0.1$ in system (10). Figure 5 shows that $E_1 = (0.9171, 0.0801, 0)$ is globally asymptotically stable.

In fact, $\tau = 0.3815$ is a critical value of rumor propagation in this case. For example, when $\tau = 0.3 < 0.3815$ rumor begins to prevail in the online social network, and when $\tau = 0.45 > 0.3815$ there are no infected users, as shown in Fig. 6. Thus, the latent period can determine whether the rumor spreads or not to some extent. Obviously, larger latent period is helpful to eliminate rumors. This is well understood. The network rumor is a real-time information. If there are no users to forward rumors for a long time, rumors may no longer be concerned.

C. Stability of the interior equilibrium point E_2

Consider $L = 5, d = 5, \beta_1 = 0.35, \beta_2 = 0.38, \mu = 0.3, \alpha = 0.6$, and $\tau = 0.1$ in system (10). A simple calculations show that $\mathscr{R}_1 = 1.6668 > 1$ and then the interior equilibrium point $E_2 = (0.5570, 0.2632, 0.1755)$ is globally asymptotically stable from Theorem 8, as shown in Fig. 7. That is to say, the densities of susceptible users, infected users, and recovered users are 0.5570, 0.2632,

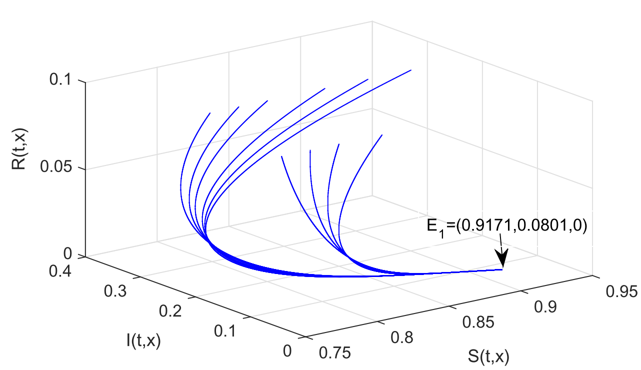

FIG. 5. equilibrium point E_1 is globally asymptotically stable.

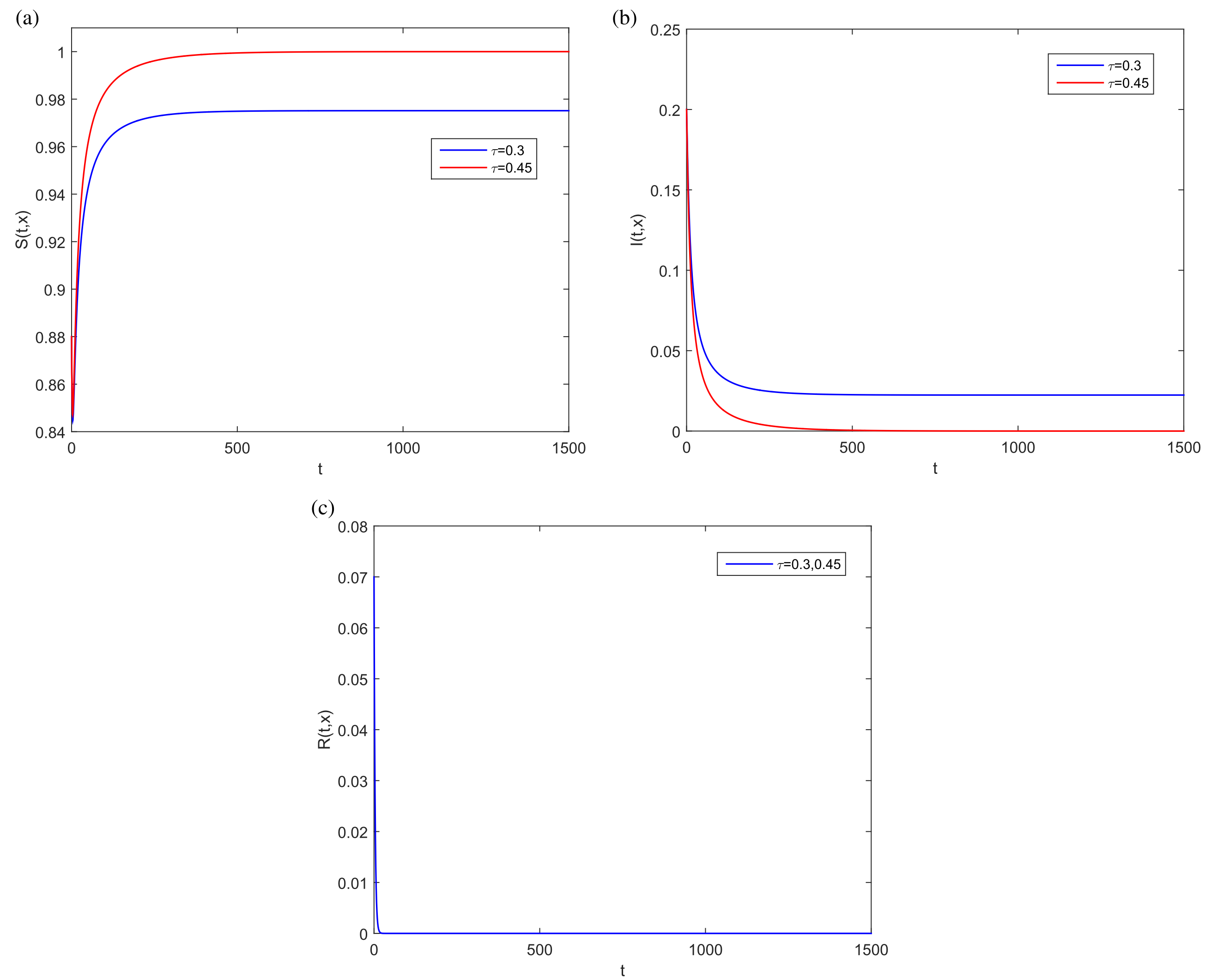

FIG. 6. The densities of susceptible users, infected users, and recovered users for $\tau = 0.3$ and $\tau = 0.45$, respectively.

and 0.1755 at the final state of rumor propagation, respectively. Obviously, the value of $\mathscr{R}_1$ is a key factor in this case, which decides whether the three kinds of users can coexist in an online social network. In other words, $\mathscr{R}_1$ determines the final state of rumor propagation.

The contour plots of Fig. 8(a) show the dependence of $\mathscr{R}_1$ on the time delay τ and the rumor transmission rate β_1. From Fig. 8(a), we know that by controlling values of τ and β_1 in regions I–III, we can guarantee that susceptible users, infected users, and recovered users do not co-exist in an online social network, which is the first step to eliminate rumor propagation. However, it is not enough. From Fig. 8(b), which is the contour plots of $\mathscr{R}_0$, we find that in the part of region II and the whole region III, there still exist infected users even without any recovered users. That is to say, rumor can continue spreading in this situation. Thus, in order to completely terminate rumor diffusion, we must choose τ and β_1 in region I of Fig. 8(b).

D. The influence of parameter μ on rumor propagation

The exit rate μ sometimes has a significant impact on rumor propagation. First, we consider the interrelation among μ, $\mathscr{R}_0$, and $\mathscr{R}_1$. A direct calculation shows that

$$\frac{d\mathscr{R}_0}{d\mu} = -\frac{\beta_1}{\mu} e^{-\mu\tau} \left(\frac{1}{\mu} + \tau \right) < 0$$

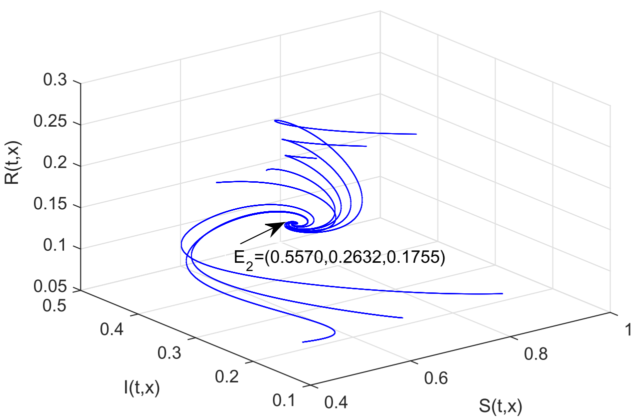

FIG. 7. The interior equilibrium point E_2 is globally asymptotically stable.

and

$$\frac{d\mathscr{R}_1}{d\mu} = -\frac{\beta_1\beta_2}{\mu(\beta_1+\beta_2+\mu\alpha)}e^{-\mu\tau}\left(\tau+\frac{1}{\mu}+\frac{\alpha}{\beta_1+\beta_2+\mu\alpha}\right) < 0.$$

Obviously, $\mathscr{R}_0$ and $\mathscr{R}_1$ are both monotone decreasing functions about the exit rate μ, as shown in Fig. 9 (here, $\beta_1 = 0.4, \beta_2 = 0.15$, $\alpha = 0.3, \tau = 7.5, \mu \in [0.01, 0.4]$). In this work, $\mathscr{R}_0$ and $\mathscr{R}_1$ are the key indexes for rumor propagation. The research shows that increasing the exit rate μ is an effective method to satisfy $\mathscr{R}_0 < 1$ and $\mathscr{R}_1 < 1$. That is to say, if the government strengthens the education of network users when rumor spreads such that more users drop out of rumor propagation (namely, enlarge the exit rate μ), then rumor may halt diffusion.

Furthermore, keeping the above parameters unchanged, we analyze the influence of the exit rate μ on the density of rumor infected users. Figure 10 shows that when the exit rate μ is smaller, the density of rumor infected users will increase with μ increasing. However, when μ increases to a certain value, for example, $\mu = 0.0648$, the density of rumor infected users is rapidly reducing until $\mu = 0.1400$ and after that there no longer exist any rumor infected users. Why the density of rumor infected users will increase when μ is smaller enough and $\mu \in [0.0100, 0.0648]$. Meanwhile, why the density of rumor infected users is decreasing for $\mu \in [0.0648, 0.1400]$ and after that there are no rumor infected users. In fact, when $\mu \in [0.0100, 0.0648]$, we can calculate that $\mathscr{R}_1 > 1$. That is to say, the interior equilibrium point E_2 is globally asymptotic stability. Thus, according to the global stability of E_2, the density of rumor infected users in social networks is $\frac{\mu}{\beta_2}$ in the end. Clearly, it is a monotone increasing function about μ, which is consistent with Fig. 10. Moreover, we find that $\mathscr{R}_0 > 1$ and $\mathscr{R}_1 \leq 1$ when $\mu \in [0.0648, 0.1400]$. Thus, E_1 is globally asymptotic stability. Following $\frac{dI}{d\mu} = -\frac{(1+\beta_1\tau e^{-\mu\tau})(\beta_1+\mu\alpha)+\mu(\mathscr{R}_0-1)}{(\beta_1+\mu\alpha)^2} < 0$, the density of rumor infected users has decreasing property with μ when E_1 is globally stable. Looking still further ahead, $\mathscr{R}_0$ is less than or equal to 1 for $\mu > 0.1400$, namely, E_0 is globally stable. Therefore, there are no rumor infected users in the end. Figure 10 shows that only

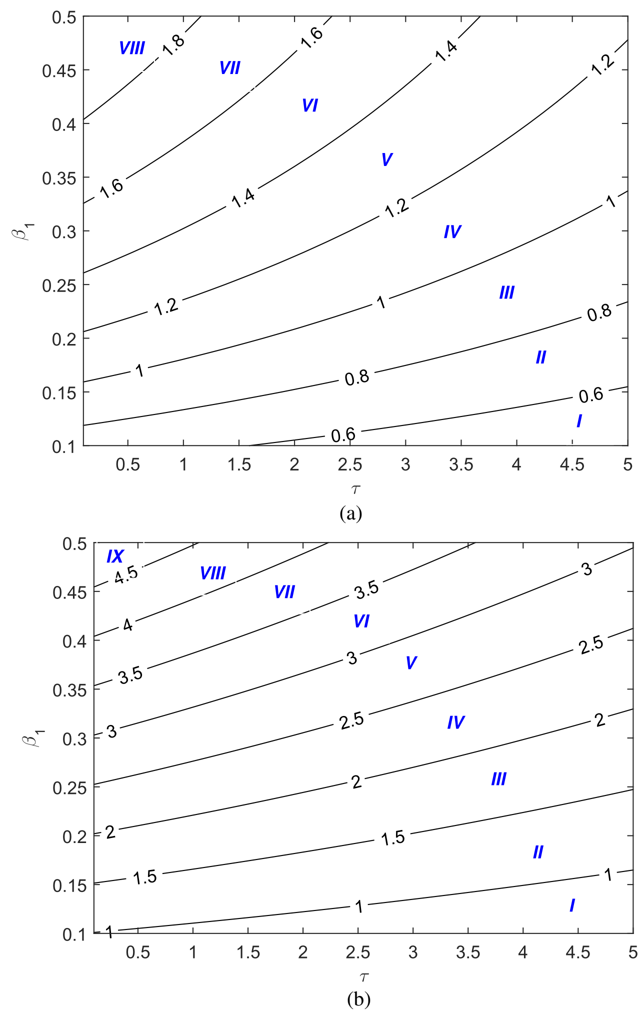

FIG. 8. (a) Contour plots of $\mathscr{R}_1$ with consideration of $L = 5, d = 1$, $\alpha = 0.5, \mu = 0.1, \beta_2 = 0.38, \beta_1 \in [0.1, 0.5]$, and $\tau \in [0.1, 5]$. (b) Contour plots of $\mathscr{R}_0$ with consideration of $L = 5, d = 1, \alpha = 0.5, \mu = 0.1, \beta_2 = 0.38, \beta_1 \in [0.1, 0.5]$, and $\tau \in [0.1, 5]$.

when μ is small and $\mu = 0.0648$, the density of rumor infected users can reach its maximum, and it further fully testifies that larger exit rate μ is helpful to eliminate rumor propagation in social networks.

VI. COMPARATIVE ANALYSIS

Example 1. In system (10), we consider the effect of an exit rate on the latent period by introducing $e^{-\mu\tau}$. What will happen if there is no term $e^{-\mu\tau}$. Now, we establish a new model without consideration of the effect of an exit rate on the latent period as

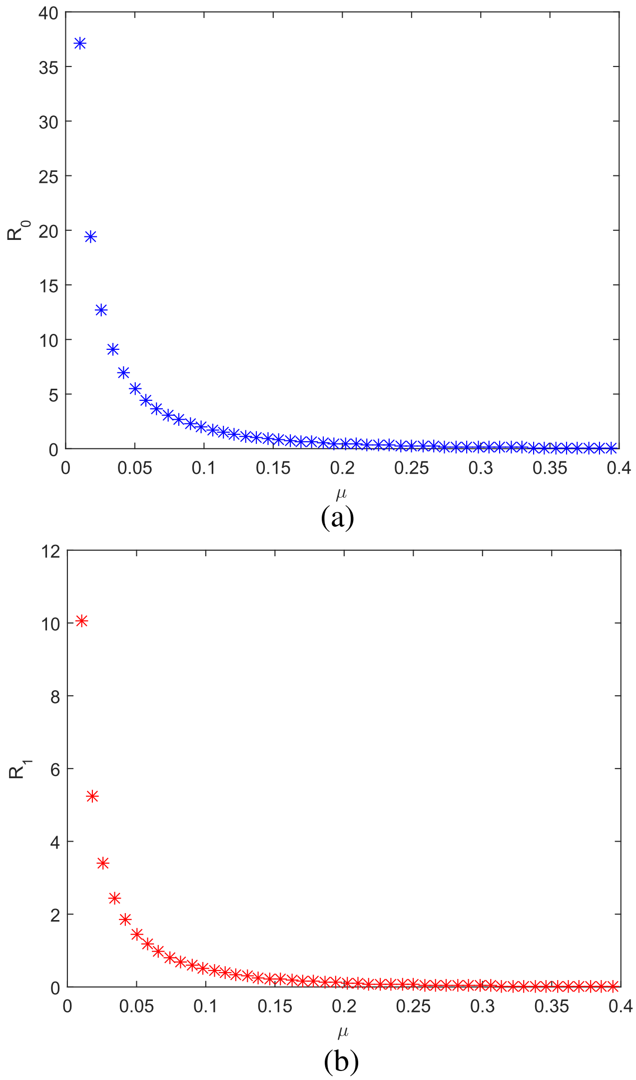

FIG. 9. (a) The interrelation between μ and $\mathscr{R}_0$. (b) The interrelation between μ and $\mathscr{R}_1$.

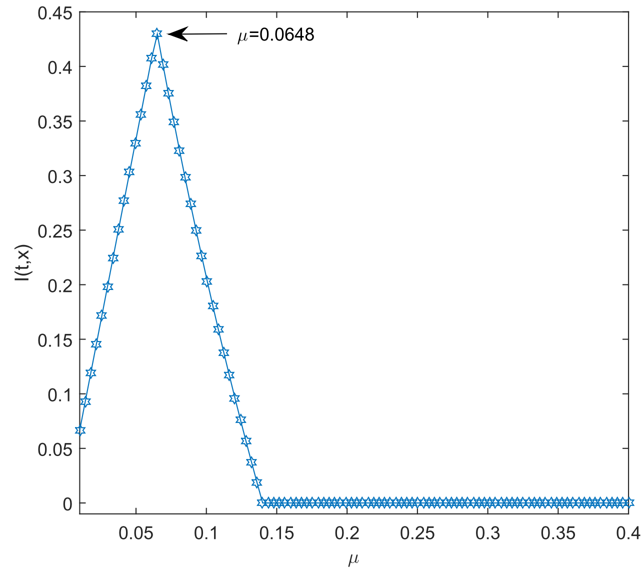

FIG. 10. The density of rumor infected users varies with μ increasing.

follows:

$$\begin{cases} \dfrac{\partial S(t,x)}{\partial t} = d\Delta S(t,x) + \mu - \dfrac{\beta_1 S(t,x) I(t,x)}{1+\alpha I(t,x)} - \mu S(t,x), \\ \dfrac{\partial I(t,x)}{\partial t} = d\Delta I(t,x) + \dfrac{\beta_1 S(t-\tau,x) I(t-\tau,x)}{1+\alpha I(t-\tau,x)} \\ \qquad -\beta_2 I(t,x) R(t,x) - \mu I(t,x), \\ \dfrac{\partial R(t,x)}{\partial t} = d\Delta R(t,x) + \beta_2 I(t,x) R(t,x) - \mu R(t,x). \end{cases} \tag{53}$$

In the following, we will compare the different dynamic characteristics of system (53) and system (10). Without loss of generality, take $L = 5, d = 2, \beta_1 = 0.3, \beta_2 = 0.18, \mu = 0.18, \alpha = 0.6$, and $\tau = 6$ in system (53) and system (10). As Fig. 11(a) shows, there exist rumor infected users in social networks. That is to say, rumor continues spreading when we do not think about the effect of an exit rate on the latent period. On the other hand, Fig. 11(b) shows that there are no any infected users and recovered users. In other words, under the same parameters with system (53), the effect of an exit rate on the rumor propagation latent period can eliminate rumor propagation. Thus, the rumor infection rate with an exponential decay directly affects whether the rumor spreads in social networks.

Example 2. In Ref. 13, Wang *et al.* first studied information transmission over both temporal and spatial scales in online social networks. They defined spatial distance of information diffusion by using friendship hops. That is to say, according to friendship hops a social network user population U can be decomposed into a set of groups, i.e., $U = \{U_1, U_2, \ldots, U_m\}$, where m is the maximum diffusion distance. Obviously, this definition method of spatial distance can only capture the dynamics characteristic of information diffusion at the distance $x = 1, 2, 3 \ldots$. But how about $x = 0.5$ or $x = 1.5$? In other words, the above definition is based on a discrete space and information diffusion cannot be described by a continuous reaction-diffusive mathematical model. However, information diffusion usually is continuous either on temporal scale or on spatial scale in social networks. In our work, we use *cluster importance* to define spatial distance of information diffusion. That is to say, the more important the users are, the closer it gets to the source of information by the users. For example, $x \in [0, 1]$ denotes a kind of most important cluster, who are closer to information. A new definition of continuous spatial distance of information diffusion is given in this work, and it makes up for the deficiency of Ref. 13 about the definition of discrete spatial distance of information diffusion. Meanwhile, our work has revealed a final state of rumor propagation by analyzing the global

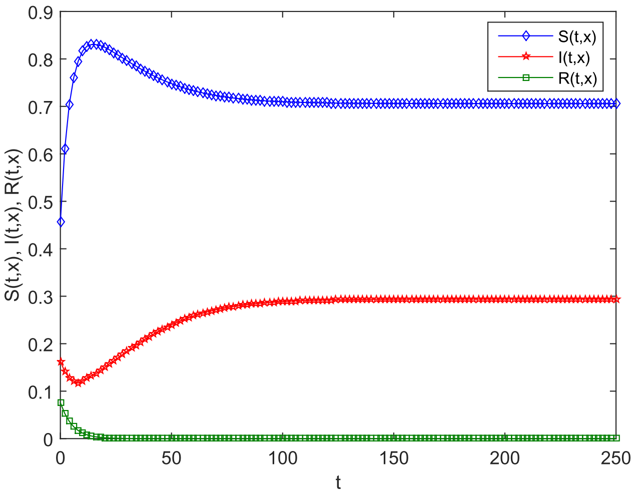

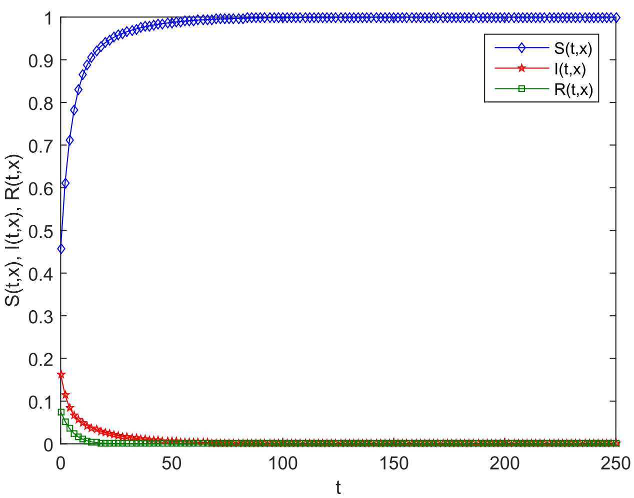

FIG. 11. The density of susceptible users, infected users, and recovered users. (a) System (53). (b) System (10).

stability of a delayed reaction-diffusion rumor propagation model in social networks, which expands the theoretical analysis of Ref. 13.

VII. CONCLUSION AND FUTURE WORK

This paper mainly focuses on modeling rumor propagation over both temporal and spatial dimensions in online social networks. The key technical problem is to define a spatial distance of rumor propagation in online social networks. Clustering is important for modeling rumor propagation in online social networks as clustering usually can be used to define distance in social media. Thus, we have applied the approach of **k**-means to search for clusters for a simple network in Ref. 15 based on motif M_7. Then, we analyze the importance of different clusters by combining the neighbor node information, the cluster coefficient, and the average node importance evaluation index of each cluster. By using *cluster importance* as a distance, we abstractly translate the rumor propagation process in online social networks into two correlated processes: time growth process and space growth process, and then we establish a PDE mathematical model (10) with a delay to describe rumor propagation over both temporal and spatial dimensions.

In model (10), different equilibrium points are obtained by defining $\mathscr{R}_0$ and $\mathscr{R}_1$. Meanwhile, when $\mathscr{R}_0 \leq 1$, the infection-free equilibrium point E_0 of system (10) is globally asymptotically stable. Otherwise, E_0 is unstable. When $\mathscr{R}_0 > 1$ and $\mathscr{R}_1 \leq 1$, equilibrium point E_1 is globally asymptotically stable, and it is unstable for $\mathscr{R}_1 > 1$. Further, if $\mathscr{R}_1 > 1$, then the interior equilibrium point E_2 is globally asymptotically stable. Numerical simulations have analyzed the possible influence factors on rumor propagation. For example, time delay may eliminate rumor propagation.

Our PDE mathematical model has provided a new insight into studying rumor propagation in online social networks. However, a lot of problems have not been solved at present. For example, for the convenience of discussion, we only use a simple network in Ref. 15, and we only have analyzed our model from the aspect of theory without consideration of the big data. These problems are also interesting and we will further discuss them in the future.

ACKNOWLEDGMENTS

The work was partially supported by the National Natural Science Foundation of China under Grant No. 11571170.

REFERENCES

[1]L. Xia, G. Jiang, B. Song, and Y. Song, "Rumor spreading model considering hesitating mechanism in complex social networks," Physica A **437**, 295–303 (2015).
[2]X. Zhao and J. Wang, "Dynamical model about rumor spreading with medium," Discrete Dyn. Nat. Soc. **2013**, 586867 (2013).
[3]H. Zhao and L. Zhu, "Dynamic analysis of a reaction-diffusion rumor propagation model," Int. J. Bifurcat. Chaos **26**(6), 1650101 (2016).
[4]L. Xia, G. Jiang, Y. Song, and B. Song, "Modeling and analyzing the interaction between network rumors and authoritative information," Entropy **17**, 471–482 (2015).
[5]Q. Zhen, S. Tang, X. Zhang, and Z. Zheng, "The independent spreaders involved SIR rumor model in complex networks," Physica A **429**, 95–102 (2015).
[6]J. Wang, L. Zhao, and R. Huang, "2SI2R rumor spreading model in homogeneous networks," Physica A **413**, 153–161 (2014).
[7]L. Zhu, H. Zhao, and H. Wang, "Complex dynamic behavior of a rumor propagation model with spatial-temporal diffusion terms," Inf. Sci. **349–350**, 119–136 (2016).
[8]X. Zhao and J. Wang, "Dynamical behaviors of rumor spreading model with control measures," Abstr. Appl. Anal. **2014**, 247359 (2014).
[9]J. Wang, L. Zhao, and R. Huang, "SIRaRu rumor spreading model in complex networks," Physica A **398**, 43–55 (2014).
[10]Y. Zan, J. Wu, P. Li, and Q. Yu, "SICR rumor spreading model in complex networks: Counterattack and self-resistance," Physica A **405**, 159–170 (2014).
[11]L. Zhao, W. Xie, H. Gao, X. Qiu, and X. Wang, "A rumor spreading model with variable forgetting rate," Physica A **392**, 6146–6154 (2013).
[12]L. Huo, J. Jiang, S. Gong, and B. He, "Dynamical behavior of a rumor transmission model with Holling-type II functional response in emergency event," Physica A **450**, 228–240 (2016).
[13]F. Wang, H. Wang, and K. Xu, "Diffusive logistic model towards predicting information diffusion in online social networks," in *32nd International Conference on Distributed Computing Systems Workshops (ICDCSW)* (IEEE, 2012), pp. 133–139.

[14]F. Wang, H. Wang, K. Xu, J. Wu, and X. Jia, "Characterizing information diffusion in online social networks with linear diffusive model," in *33rd International Conference on Distributed Computing Systems (ICDCS)* (IEEE, 2013), pp. 307–316.

[15]A. Benson, D. Gleich, and J. Leskovec, "Higher-order organization of complex networks," Sciences **353**(6295), 163–166 (2016).

[16]U. Luxburg, "A tutorial on spectral clustering," Stat. Comput. **17**(4), 395–416 (2007).

[17]I. Dhillon, "Co-clustering documents and words using bipartite spectral graph partitioning," in *Proceedings of the Seventh ACM SIGKDD International Conference on Knowledge Discovery and Data Mining* (ACM, 2001), pp. 269–274.

[18]Z. Ren, F. Shao, J. Liu, Q. Guo, and B. Wang, "Node importance measurement based on the degree and clustering coefficient information," Acta Phys. Sin. **62**(12), 128901 (2013).

[19]G. Fagiolo, "Clustering in complex directed networks," Phys. Rev. E **76**, 026107 (2007).

[20]H. Smith, *Monotone Dynamical Systems: An Introduction to the Theory of Competitive and Cooperative Systems,* Mathematical Surveys and Monographs (Book 41) (American Mathematical Society, 1995), p. 174.

[21]R. Xu and Z. Ma, "Global stability of a SIR epidemic model with nonlinear incidence rate and time delay," Nonlinear Anal. Real World Appl. **10**(5), 3175–3189 (2009).

[22]Y. Wang, Z. Jin, Z. Yang, Z. Zhang, T. Zhou, and G. Sun, "Global analysis of an SIS model with an infective vector on complex networks," Nonlinear Anal. Real World Appl. **13**(2), 543–557 (2010).

[23]K. Kim, Z. Lin, and Q. Zhang, "An SIR epidemic model with free boundary," Nonlinear Anal. Real World Appl. **14**(5), 1992–2001 (2013).

[24]J. Singh, "A new analysis for fractional rumor spreading dynamical model in a social network with Mittag-Leffler law," Chaos **29**, 013137 (2019).

[25]Y. Tian and Y. Yuan, "Effect of time delays in an HIV virotherapy model with nonlinear incidence," Proc. Math. Phys. Eng. Sci. **472**(2186), 20150626 (2016).

[26]S. Wang and J. Zhao, "Multi-attribute integrated measurement of node importance in complex networks," Chaos **25**, 113105 (2015).

[27]P. Hu and T. Mei, "Ranking influential nodes in complex networks with structural holes," Physica A **490**, 624–631 (2018).

[28]L. Zhu, M. Liu, and Y. Li, "The dynamics analysis of a rumor propagation model in online social networks," Physica A **520**, 118–137 (2019).

[29]L. Zhu, G. Guan, and Y. Li, "Nonlinear dynamical analysis and control strategies of a network-based SIS epidemic model with time delay," Appl. Math. Model. **70**, 512–531 (2019).

[30]J. Hua, L. An, and Y. Li, "Bionic fuzzy sliding mode control and robustness analysis," Appl. Math. Model. **39**(15), 4482–4493 (2015).

[31]F. Zhang, J. Hua, and Y. Li, "Indirect adaptive fuzzy control of SISO nonlinear systems with input-output nonlinear relationship," IEEE Trans. Fuzzy Syst. **26**(5), 2699–2708 (2018).

[32]Y. Li, Y. Sun, J. Hua, and L. Li, "Indirect adaptive type-2 fuzzy impulsive control of nonlinear systems," IEEE Trans. Fuzzy Syst. **23**(4), 1084–1099 (2015).

[33]Y. Li and Y. Du, "Indirect adaptive fuzzy observer and controller design based on IT2T-S fuzzy model," Appl. Math. Model. **36**, 1558–1569 (2012).

[34]F. Zhang, Y. Li, and J. Hua, "Direct adaptive fuzzy control of SISO nonlinear systems with input-output nonlinear relationship," Int. J. Fuzzy Syst. **20**(4), 1069–1078 (2018).

[35]G. Cai, S. Jiang, S. Cai, and L. Tian, "Cluster synchronization of overlapping uncertain complex networks with time-varying impulse disturbances," Nonlinear Dyn. **80**(1–2), 503–513 (2015).

[36]S. Cai, P. Zhou, and Z. Liu, "Synchronization analysis of hybrid-coupled delayed dynamical networks with impulsive effects: A unified synchronization criterion," J. Franklin Inst. **352**(5), 2065–2089 (2015).

[37]M. Peng, Z. Zhang, C. Lim, and X. Wang, "Hopf bifurcation and hybrid control of a delayed ecoepidemiological model with nonlinear incidence rate and Holling type II functional response," Math. Prob. Eng. **2018**, 6052503 (2018).

[38]R. Zhang, Y. Wang, Z. Zhang, and Q. Bi, "Nonlinear behaviors as well as the bifurcation mechanism in switched dynamical systems," Nonlinear Dyn. **79**(1), 465–471 (2015).

[39]Q. Bi, S. Li, J. Kurths, and Z. Zhang, "The mechanism of bursting oscillations with different codimensional bifurcations and nonlinear structures," Nonlinear Dyn. **85**(2), 1–13 (2016).